Solid State Detectors and Experiments: Diodes, CCD, Crystals

Marco Vignati, Sapienza
SOUP 2024

Sapienza Università di Roma
Istituto Nazionale di Fisica Nucleare

Detection channels

The combination of different techniques allows one to discriminate between electron and nuclear recoils, and thus to reduce the β/γ background.

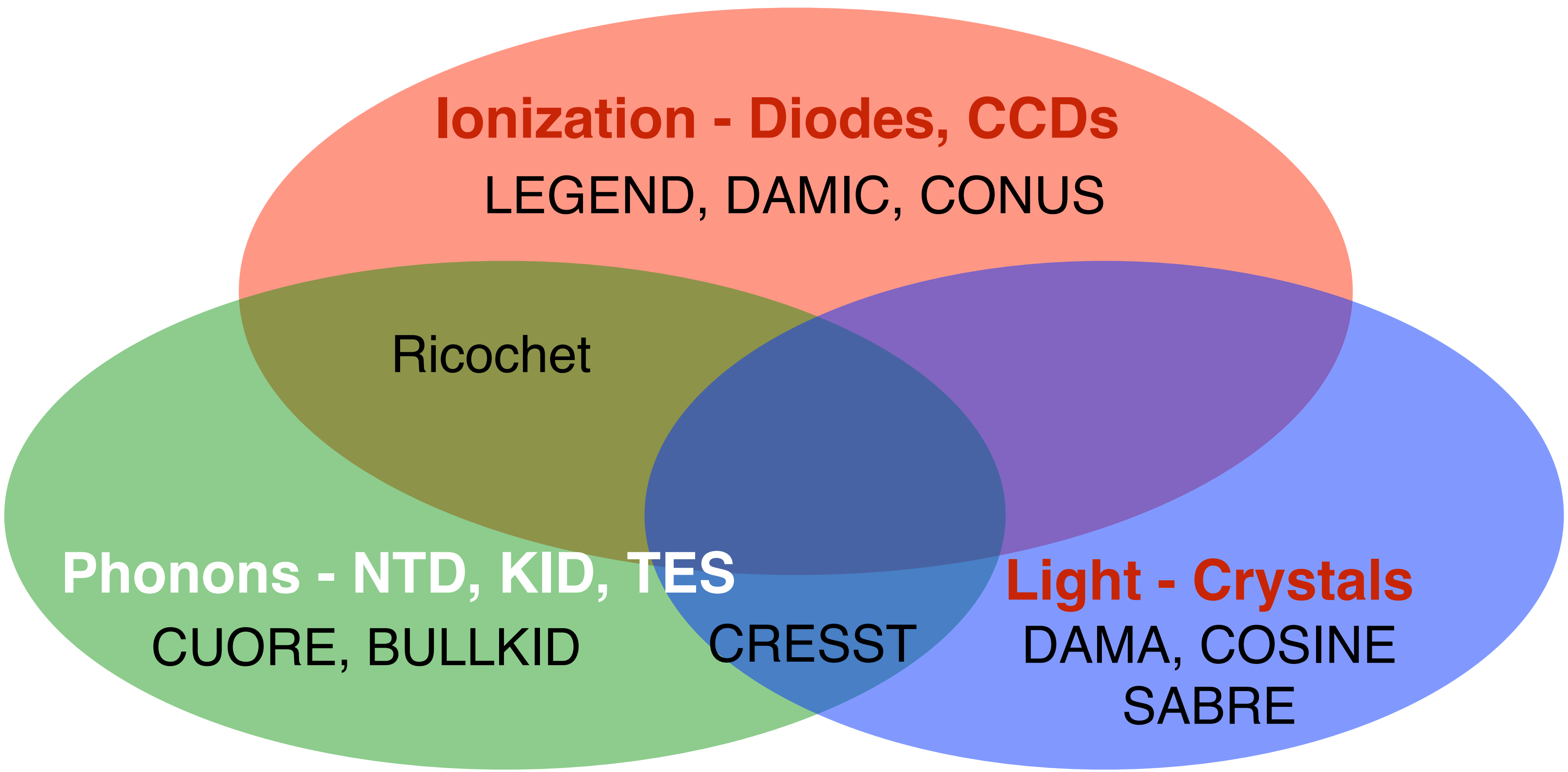

Energy calibrations are done with γ sources (electron recoils).

The relative calibration of nuclear recoils (keV_{ee} ➡ keV_{nr}), the quenching factor (QF), must be known with accuracy

Diodes

Diodes

Reversely biased p-n junction

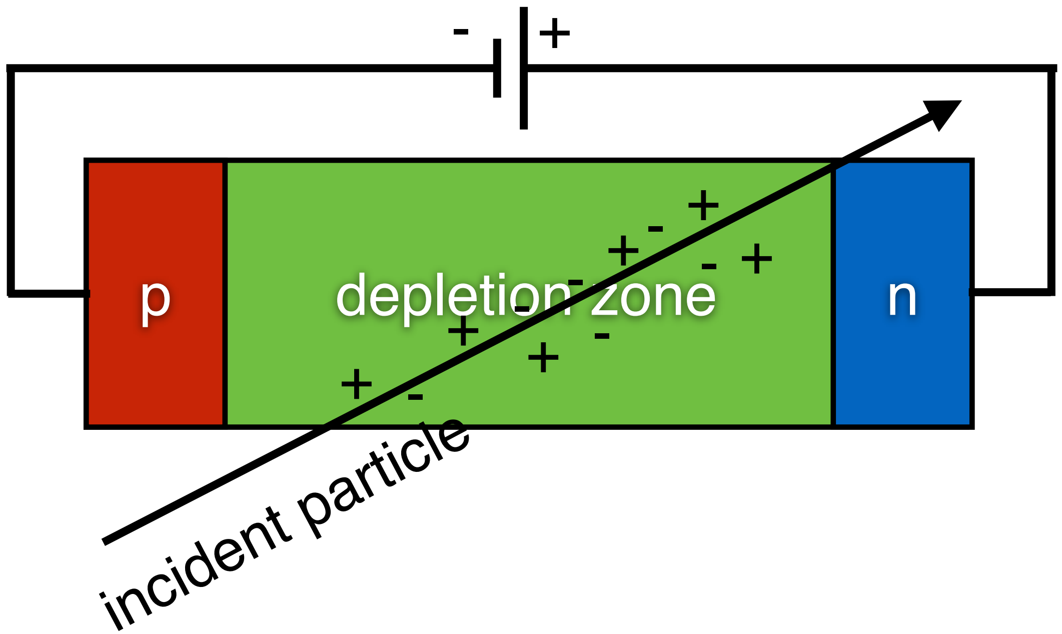

Energy (w) for e-h creation

	Si	Ge
gap	1.1 eV	0.7 eV
w 300 K	3.6 eV	-
w 77 K	3.8 eV	3.0 eV

$$\Delta E = 2.35\sqrt{wEF}, \quad F \sim 0.11$$

few keV for $E \sim$ MeV!

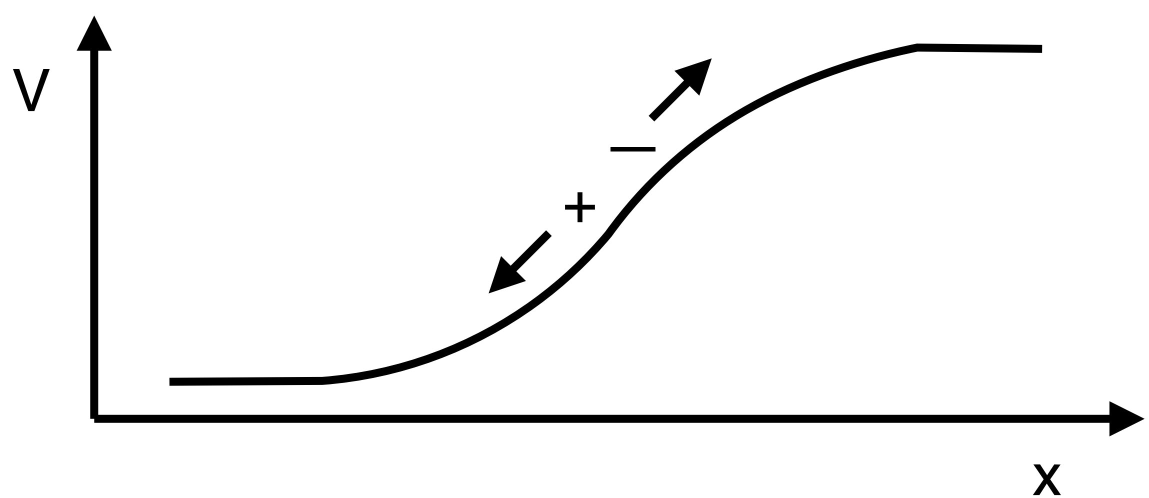

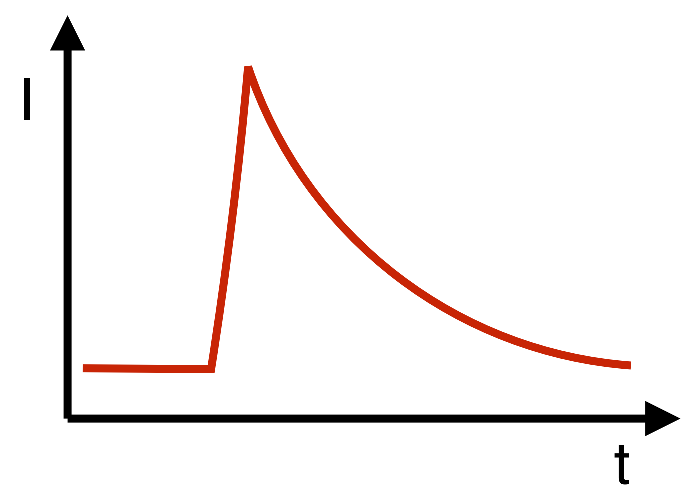

HPGe spectroscopy

- Operated at LN2 temperature

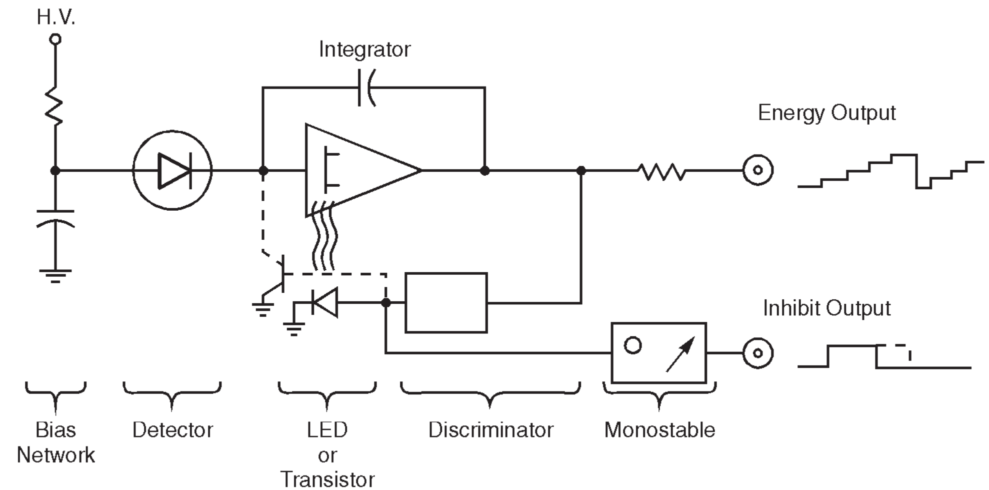

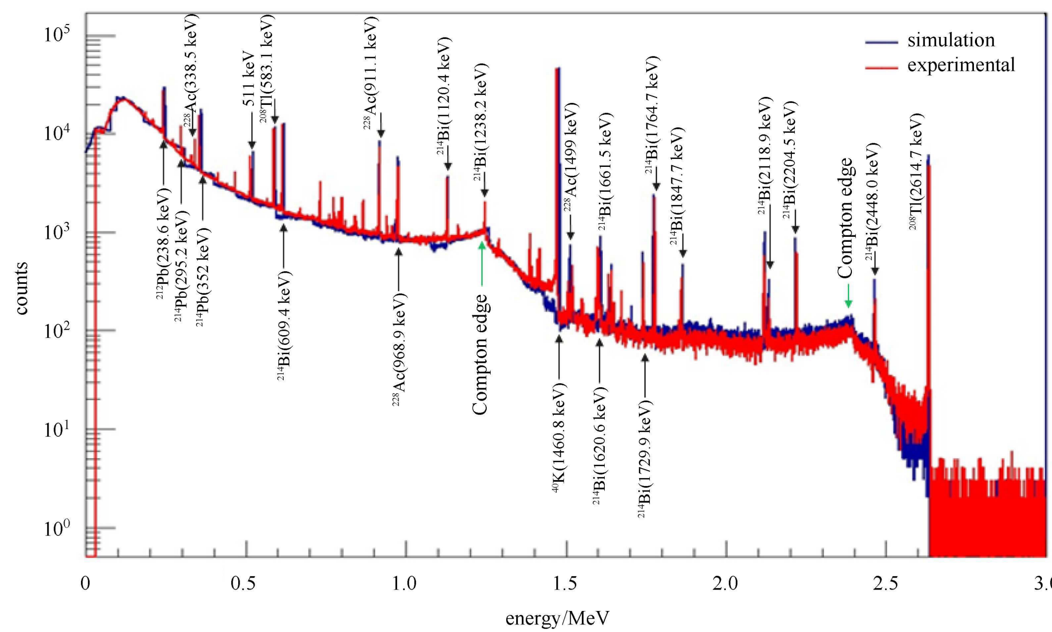

Double β decay

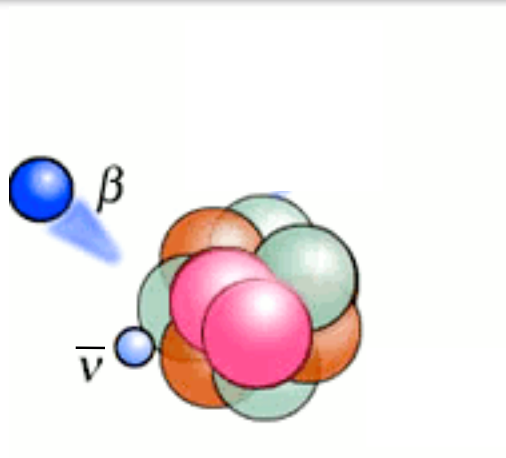

β-decay

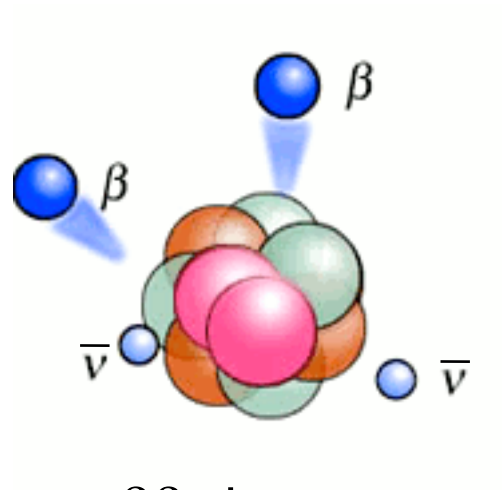

ββ-decay

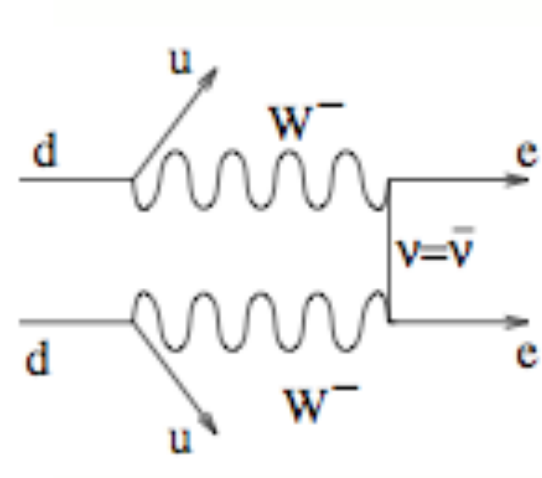

0νββ-decay

only if *νs* are Majorana

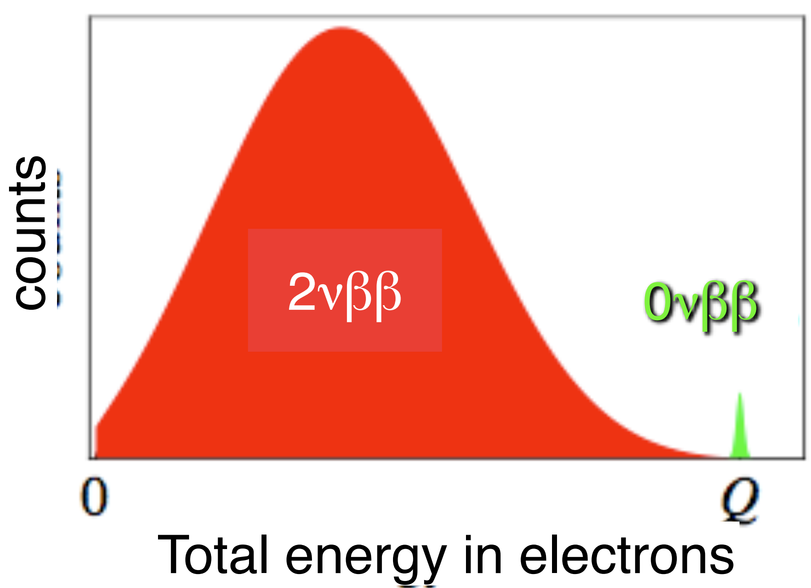

0νββ is possible only in few natural isotopes, e.g.: ^{130}Te, ^{76}Ge, ^{136}Xe,^{100}Mo,^{82}Se.

Present half-life limits are: $\tau > 10^{25\text{-}26}$ years. **Several nuclei** (100 - 1000 kg) are needed.

Almost Zero background is needed.

Excellent resolution (keV) is a very welcomed

LEGEND experiment @LNGS


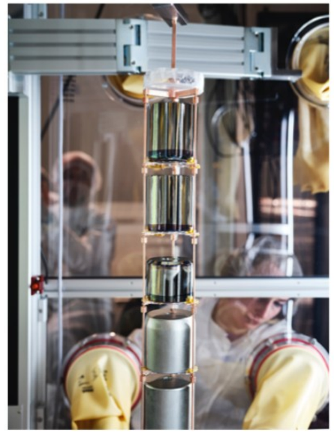

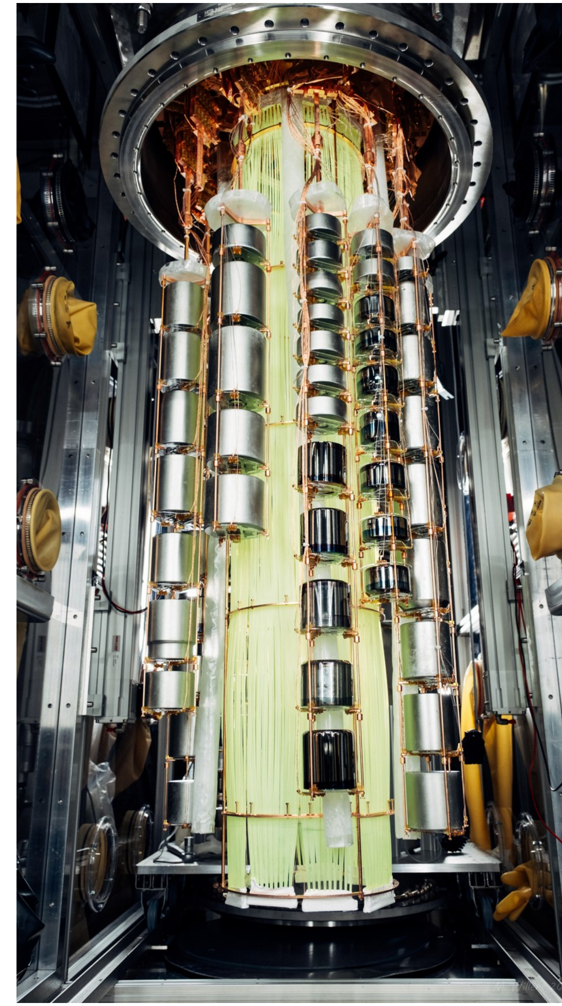
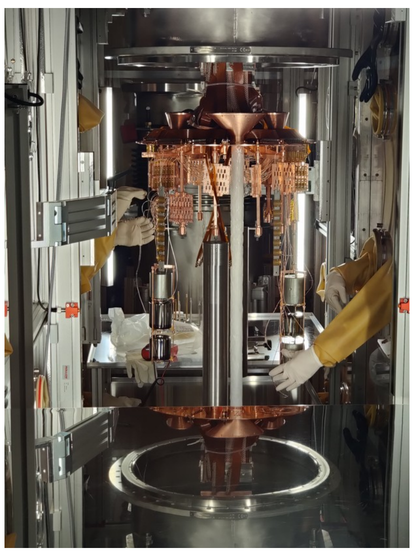
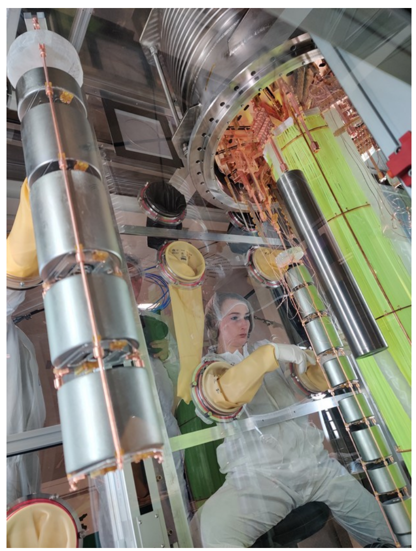
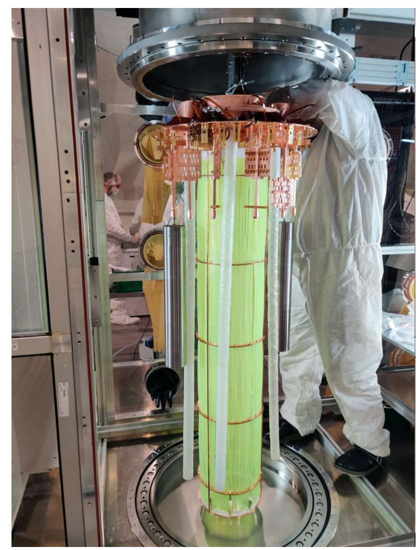

- 200 kg of ^{enr}Ge, taking physics data since 03/2023 with 142 kg of ^{enr}Ge
- Liquid Argon veto + Muon veto

Inverted coaxial HPGe

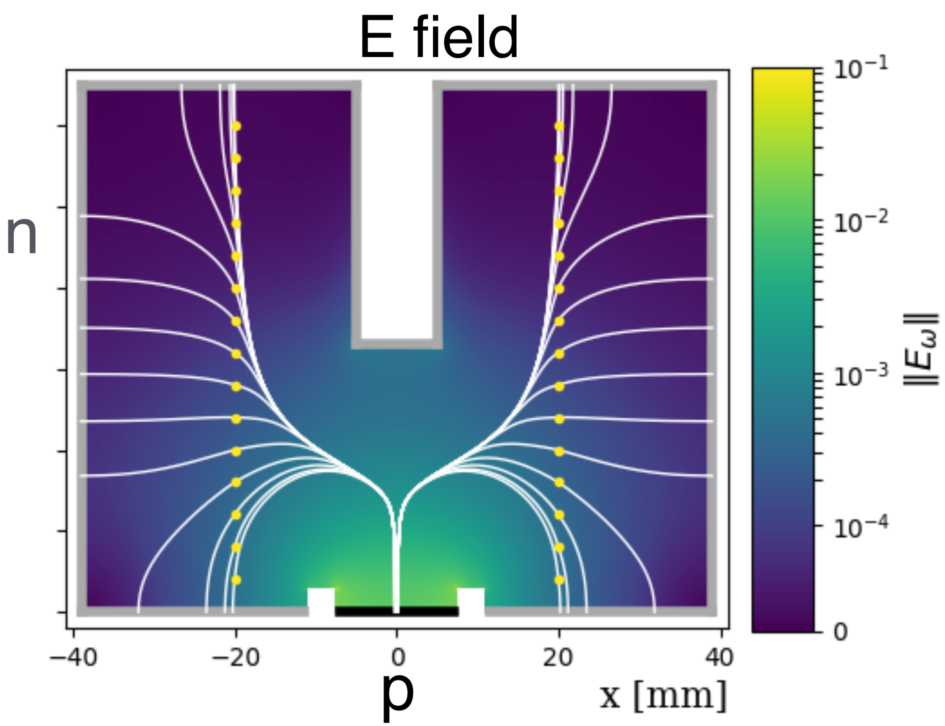

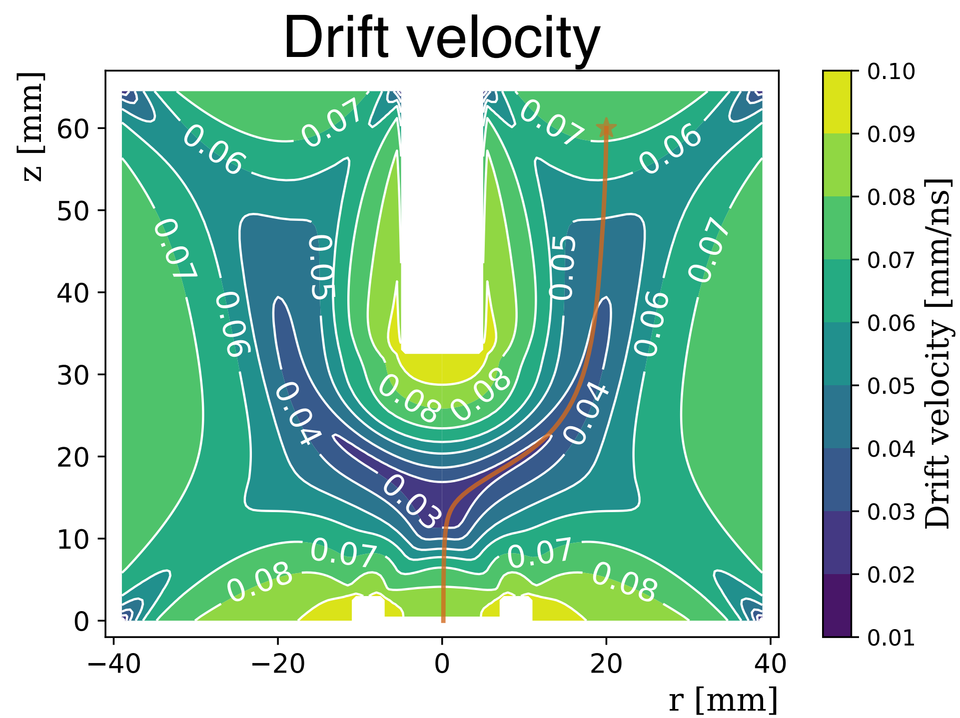

Pulse shape discrimination (PSD)

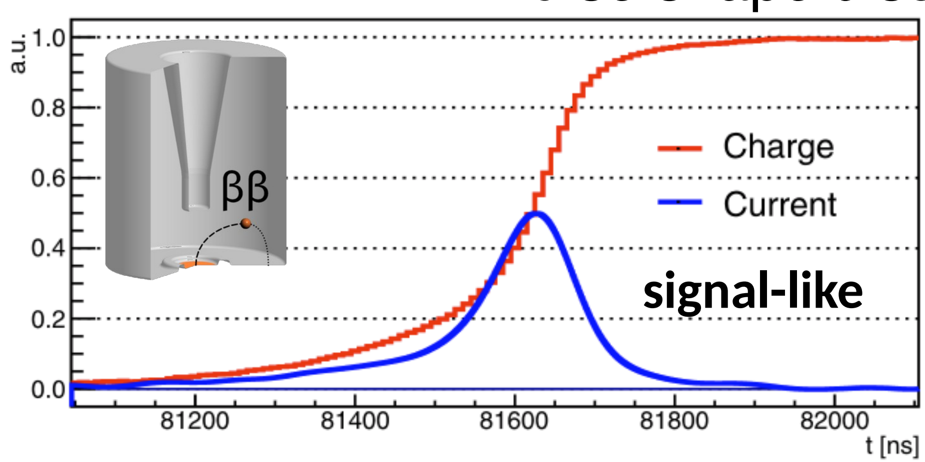

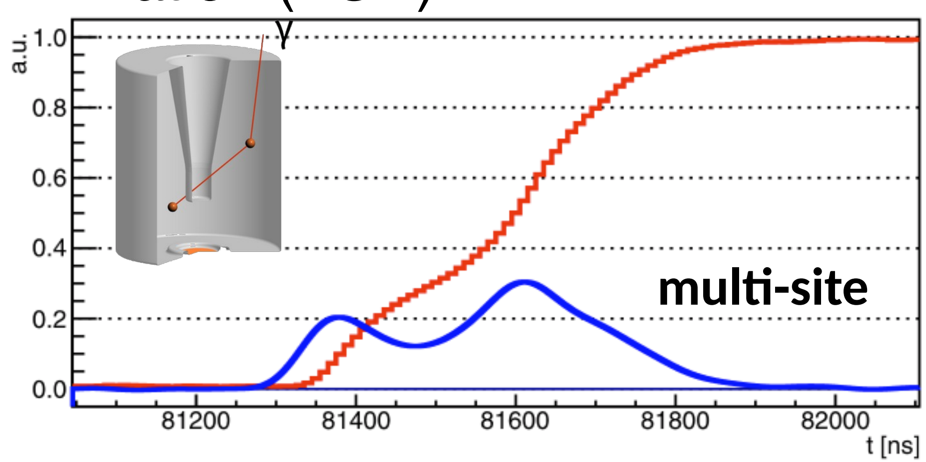

LEGEND200 @ Neutrino 2024

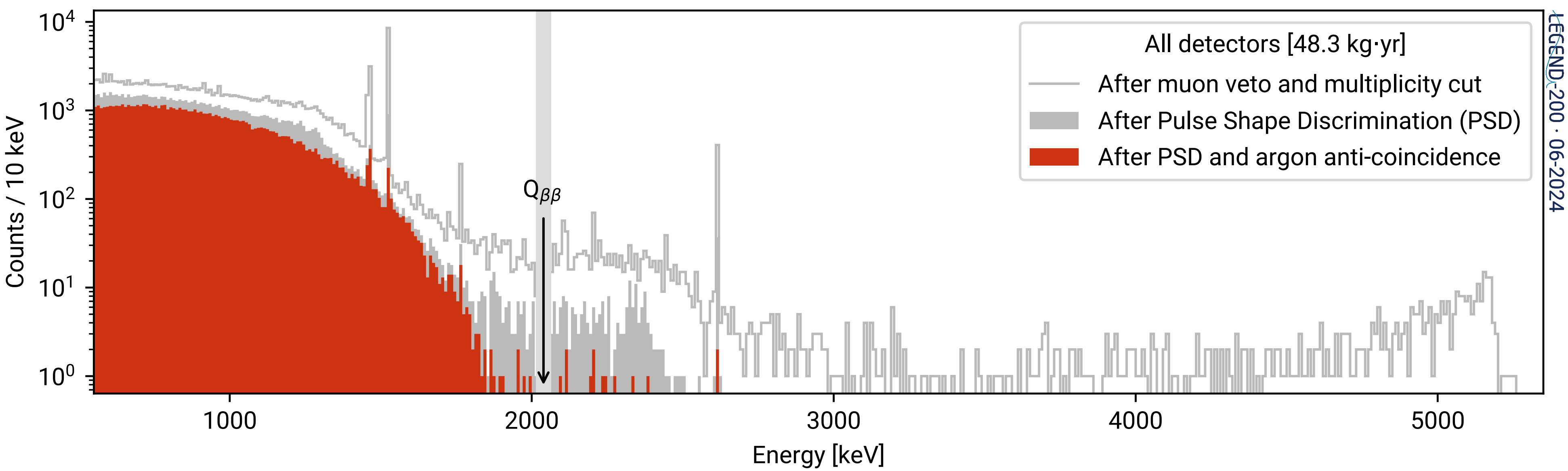

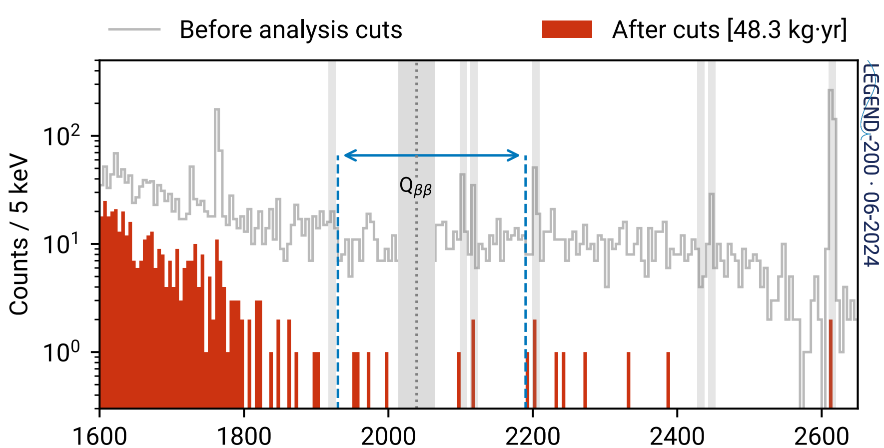

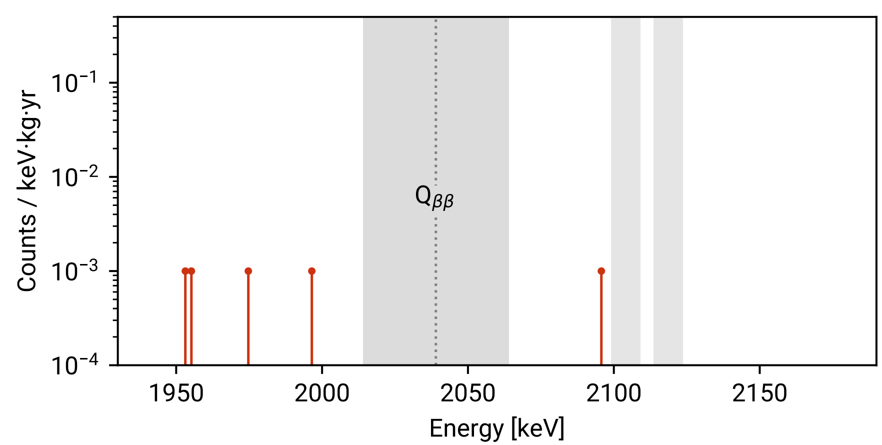

Background = (5.3 ± 2.2) x 10^{-4} cts/(keV kg yr)

$T^{0\nu}_{1/2}$ > 1.9 x 10^{26} yr (90% frequentist C.L.)

Future: LEGEND1000

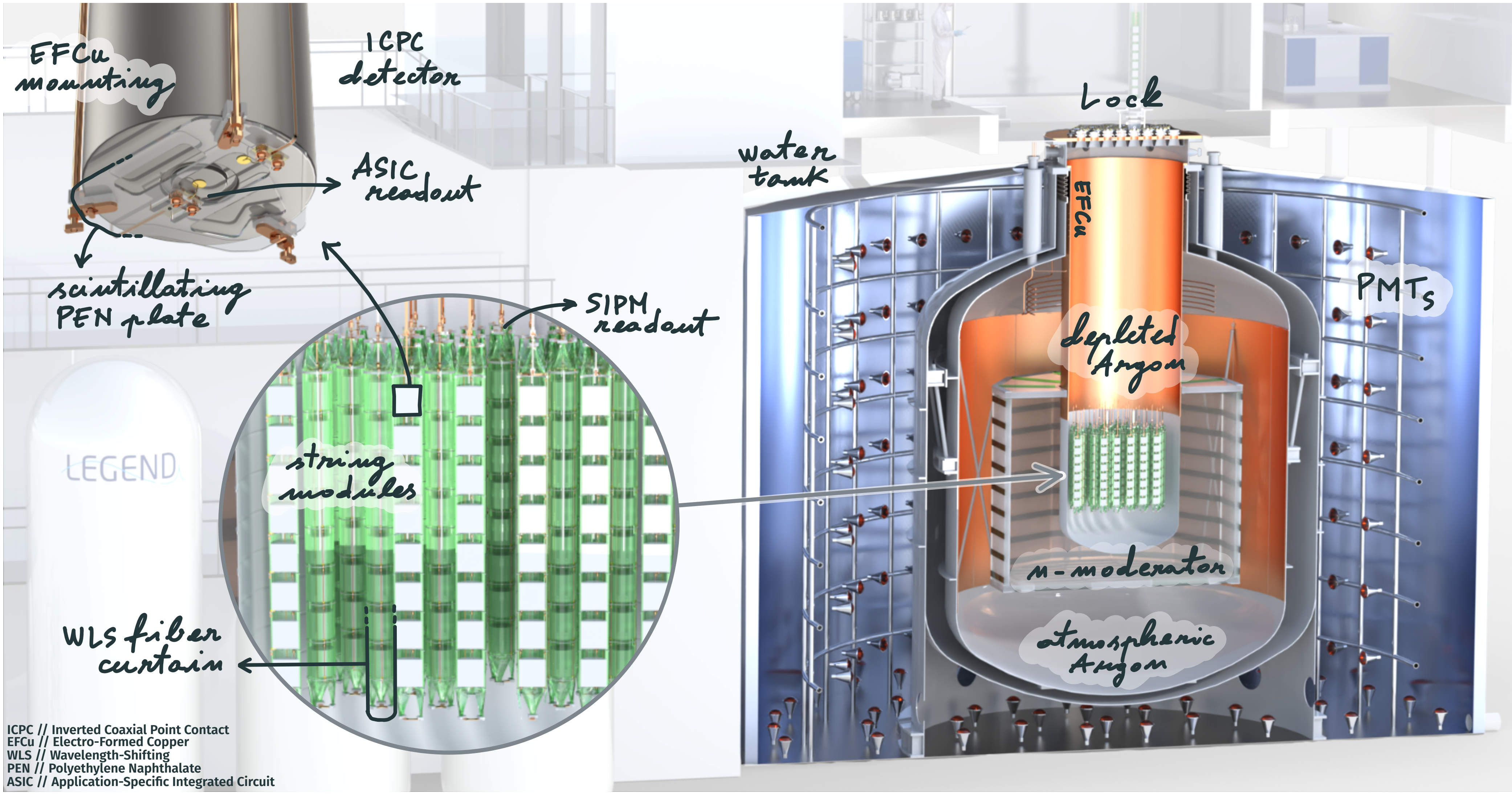

L. Pertoldi @Neutrino2024

CEνNS

Inverse Beta Decay

$$\bar{\nu} + p \to n + e^+$$

$$\sigma^0_{\mathrm{IBD}} = \frac{G_F^2 \cos^2\theta_C}{\pi}\left(f^2 + 3g^2\right) E_e p_e$$

$$E_e = E_\nu - (M_N - M_p)$$

$$E_\nu > 1.806\ \mathrm{MeV}$$

Coherent Elastic ν-Nucleus Scattering

$$\nu(\bar{\nu}) + A \to \nu(\bar{\nu}) + A$$

$$\sigma_{\mathrm{CE}\nu\mathrm{NS}} = \frac{G_F^2}{4\pi} F^2(q^2) Q_W^2 E_\nu^2$$

$$Q_W = N - Z(1 - 4\sin^2\theta_W) \sim N$$

$$E_\nu < qR$$

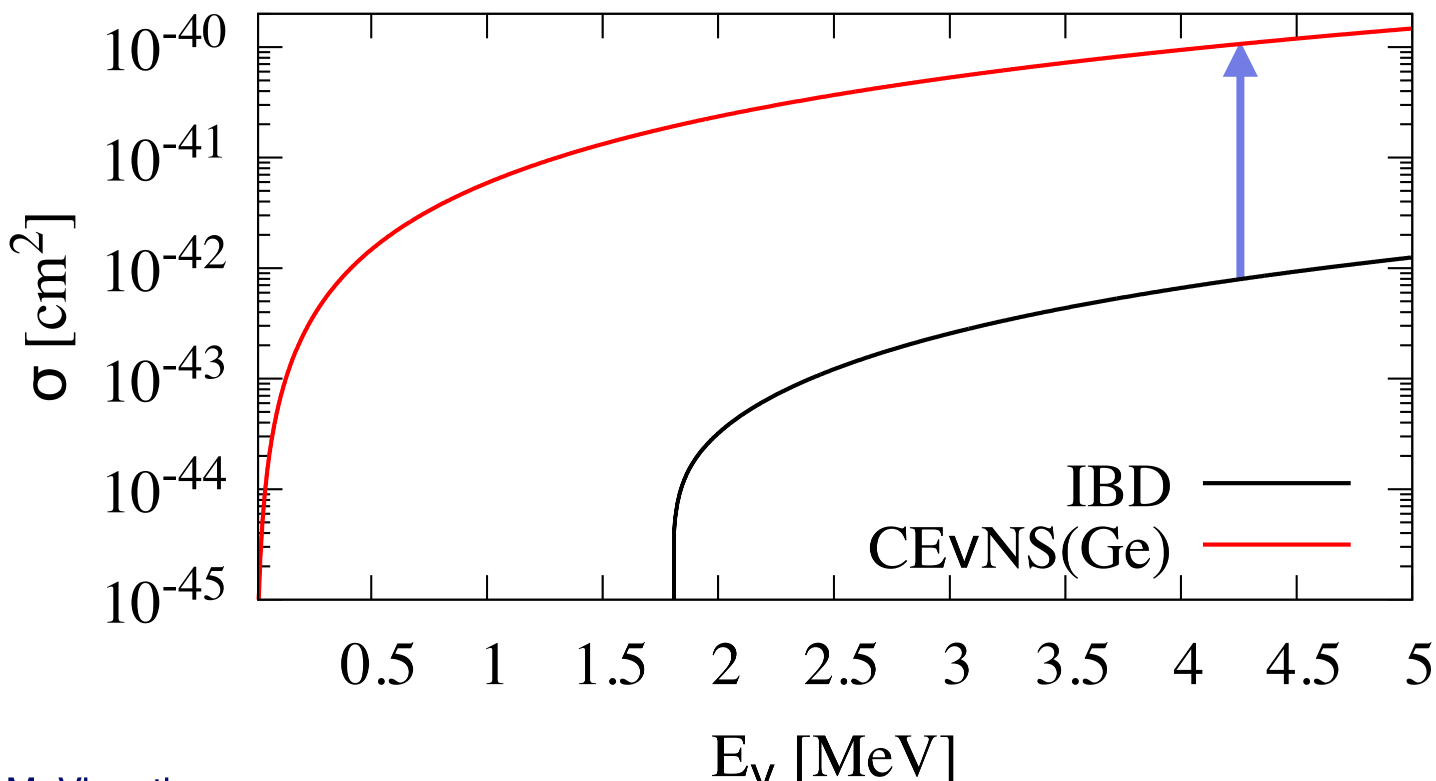

> 2 odm!

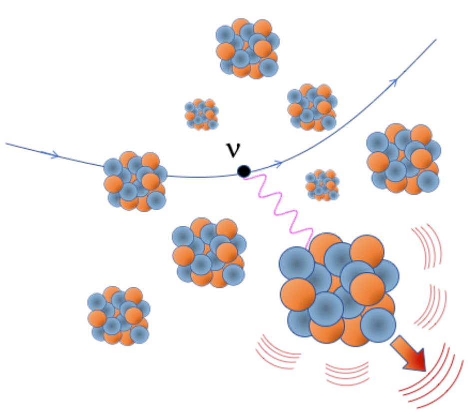

Detectable energy

Inverse Beta Decay

$$\bar{\nu} + p \to n + e^+$$

Positron energy:

$$E_e = E_\nu - (M_N - M_p)$$

Coherent Elastic ν-Nucleus Scattering

$$\nu(\bar{\nu}) + A \to \nu(\bar{\nu}) + A$$

Average nuclear recoil energy:

$$< T >= \frac{2}{3}\frac{E_\nu^2}{M_A}$$

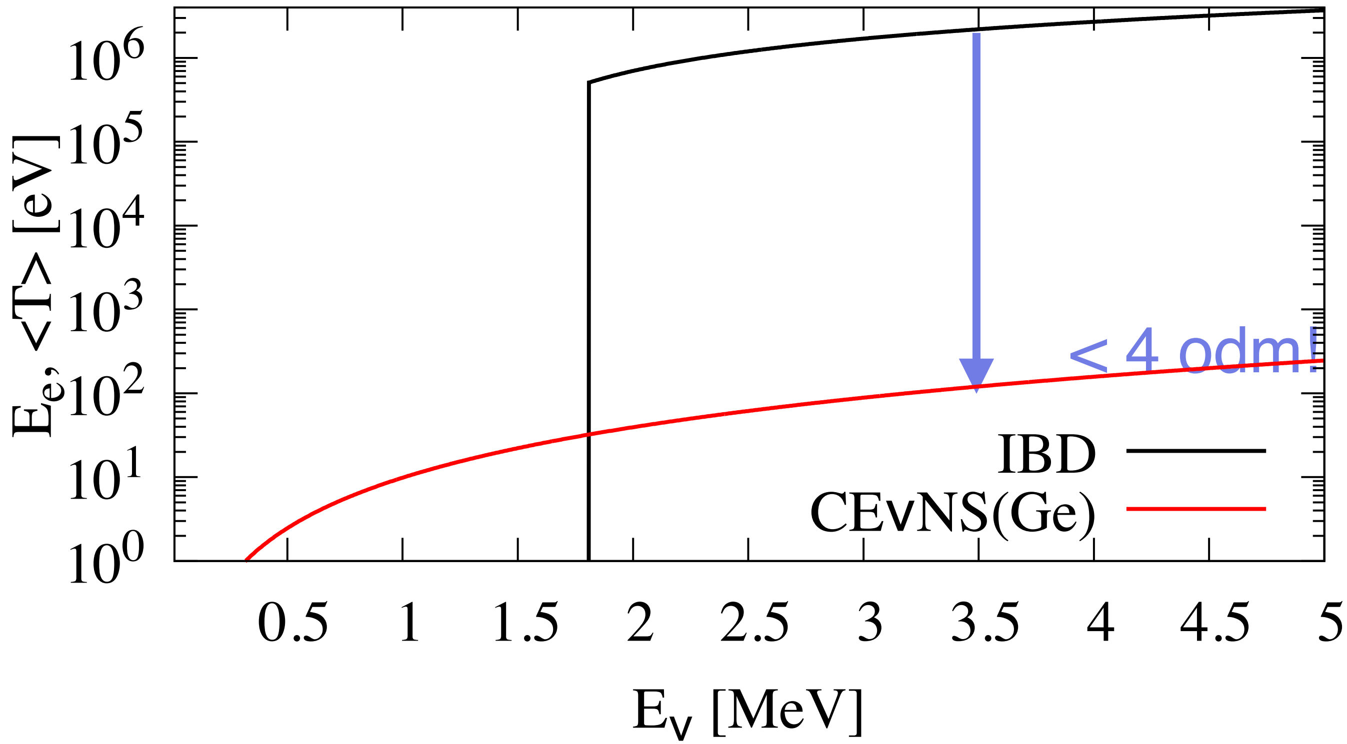

Postulated by D. Freedman in 1973

First observed by COHERENT Coll. in 2017

CONUS

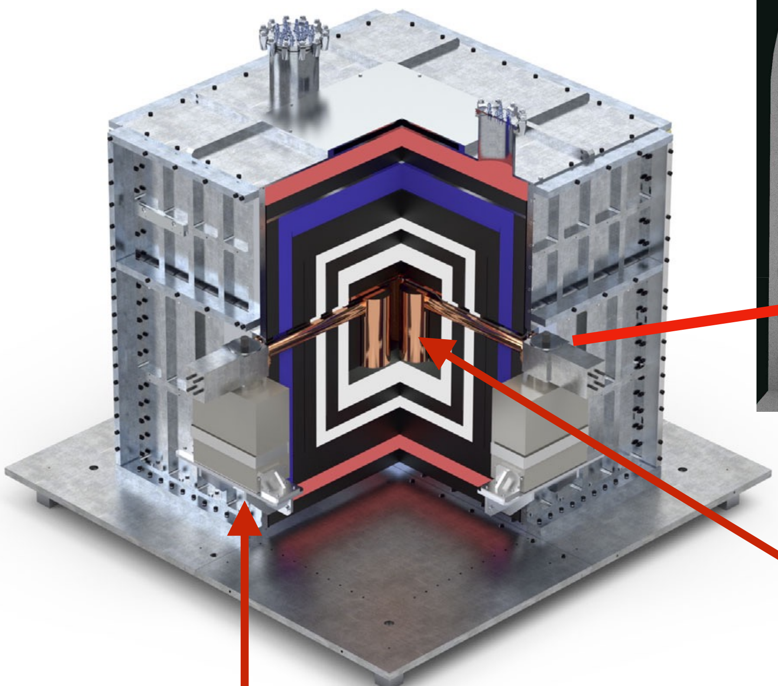

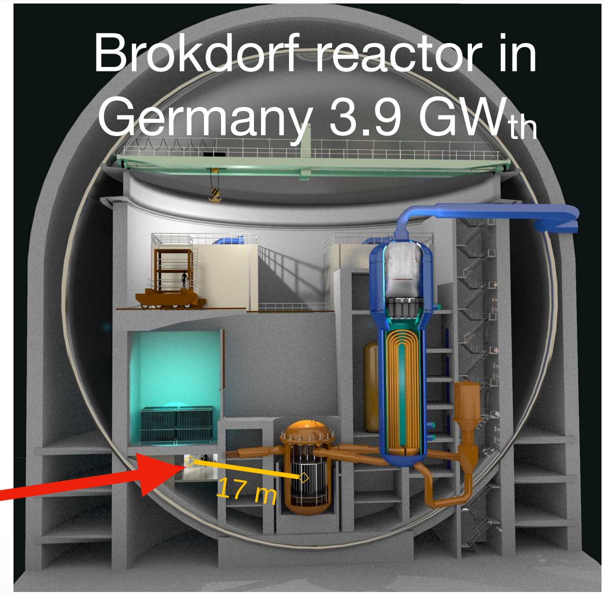

Germanium detector
Mass: 3.72 kg
baseline: 17 m
$2.3 \times 10^{13}\ \bar{\nu}/\mathrm{cm}^2\,\mathrm{s}$

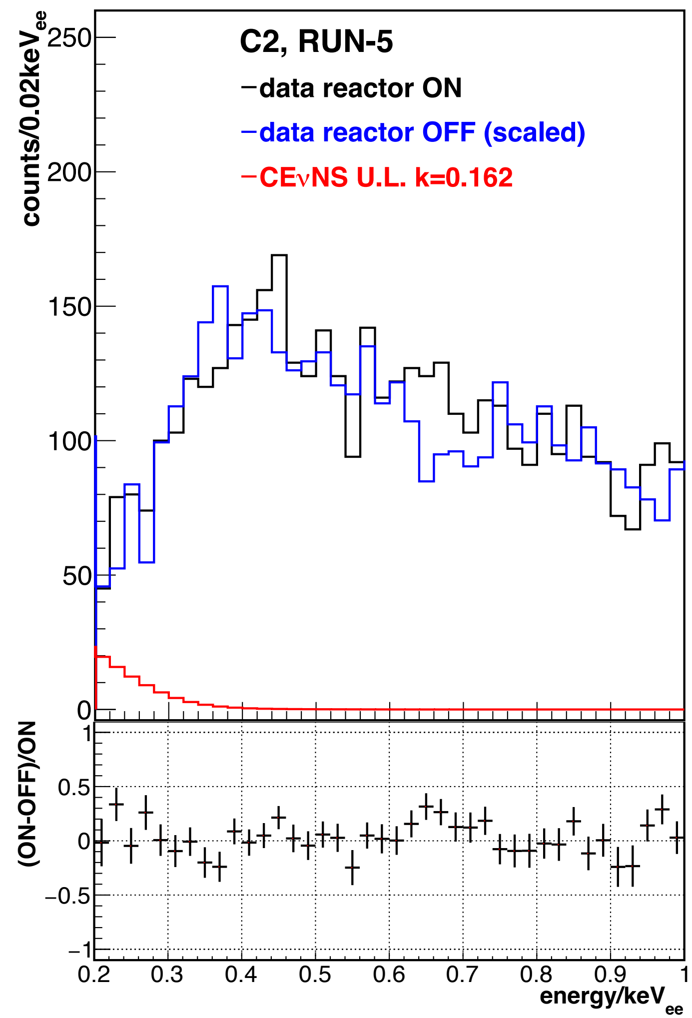

Shielding (~10 counts / keV kg d):

- Steel / Pb (black)
- Polyethilene (Red)
- B-doped PE (white)
- Plastic scintillator (blue)

Controversy on quenching

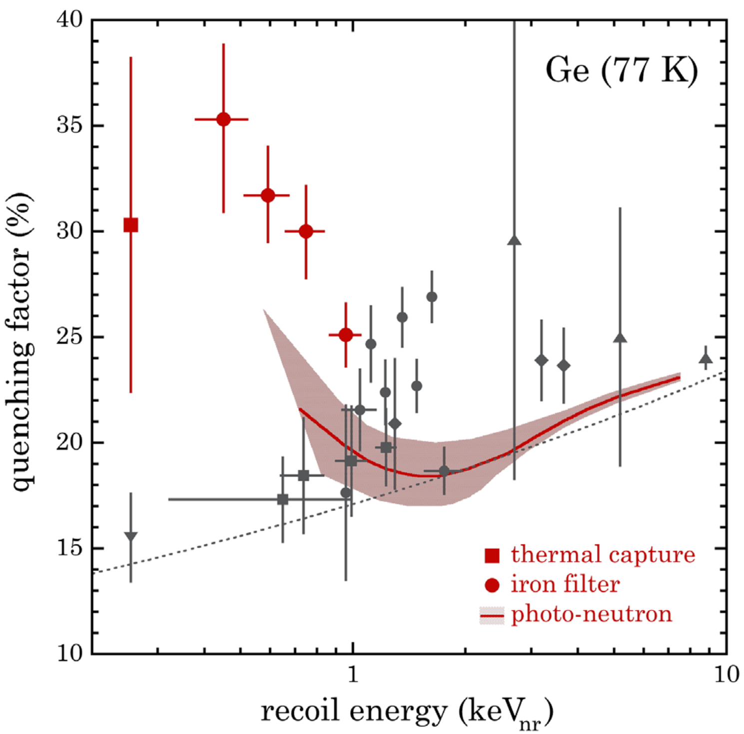

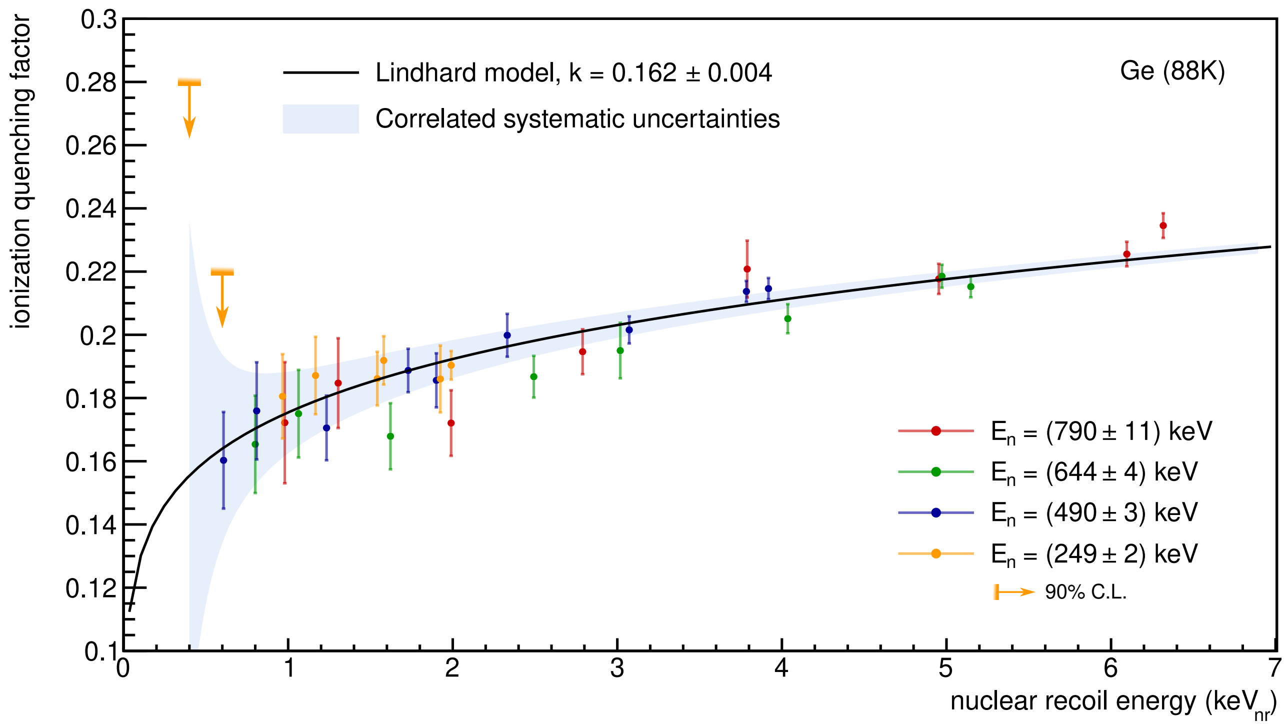

J.I. Collar, A.R.L. Kavner, and C.M. Lewis, Phys. Rev. D 103, 122003 (2021)

A. Bonhomme, et al, Eur. Phys. J. C 82, 815 (2022)

solved

CCDs

Charged Coupled Device (CCD)

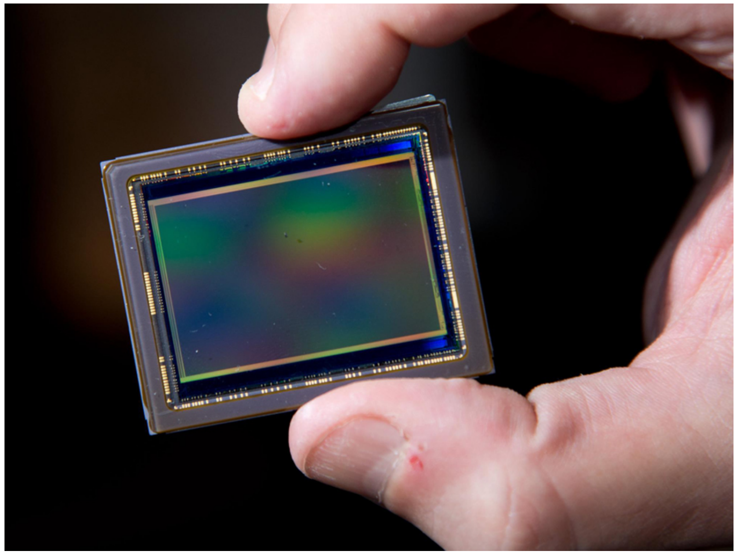

The Nobel Prize in Physics 2009

© The Nobel Foundation. Photo: U. Montan
Charles Kuen Kao
Prize share: 1/2

© The Nobel Foundation. Photo: U. Montan
Willard S. Boyle
Prize share: 1/4

© The Nobel Foundation. Photo: U. Montan
George E. Smith
Prize share: 1/4

The Nobel Prize in Physics 2009 was divided, one half awarded to Charles Kuen Kao "for groundbreaking achievements concerning the transmission of light in fibers for optical communication", the other half jointly to Willard S. Boyle and George E. Smith "for the invention of an imaging semiconductor circuit - the CCD sensor."

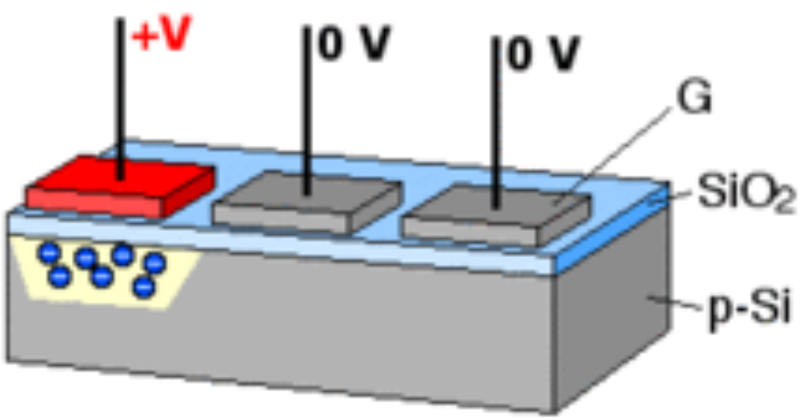

B.S.T.J. BRIEFS

Charge Coupled Semiconductor Devices

By W. S. BOYLE and G. E. SMITH

(Manuscript received January 29, 1970)

In this paper we describe a new semiconductor device concept. Basically, it consists of storing charge in potential wells created at the surface of a semiconductor and moving the charge (representing information) over the surface by moving the potential minima. We discuss schemes for creating, transferring, and detecting the presence or absence of the charge.

In particular, we consider minority carrier charge storage at the Si-SiO_2 interface of a MOS capacitor. This charge may be transferred to a closely adjacent capacitor on the same substrate by appropriate manipulation of electrode potentials. Examples of possible applications are as a shift register, as an imaging device, as a display device, and in performing logic.

https://www.nobelprize.org/prizes/physics/2009/boyle/lecture/

Charged Coupled Device (CCD)

- CCD is a *dynamic* analog (charge) shift register
- It consists of a series of MOS capacitors coupled with one another
- CCD is clocked, and all operations are in transient mode
- Charge is *coupled* from one gate to the next gate by fringing electric field, potential and carrier density gradient

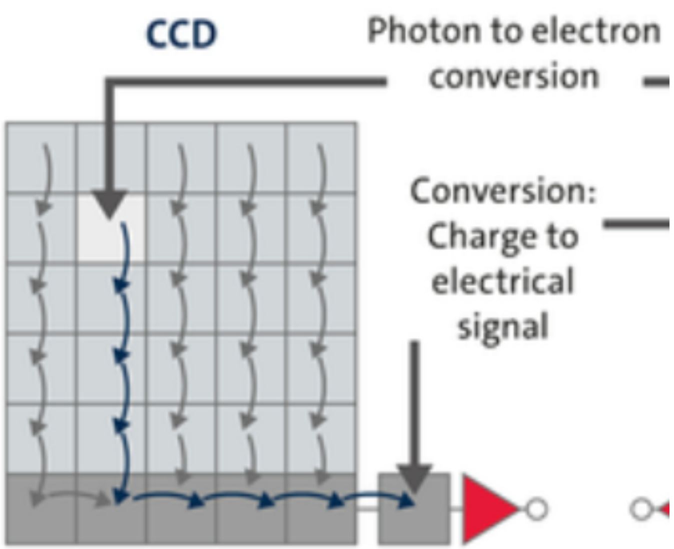

MOS capacitor

(a)

(b)

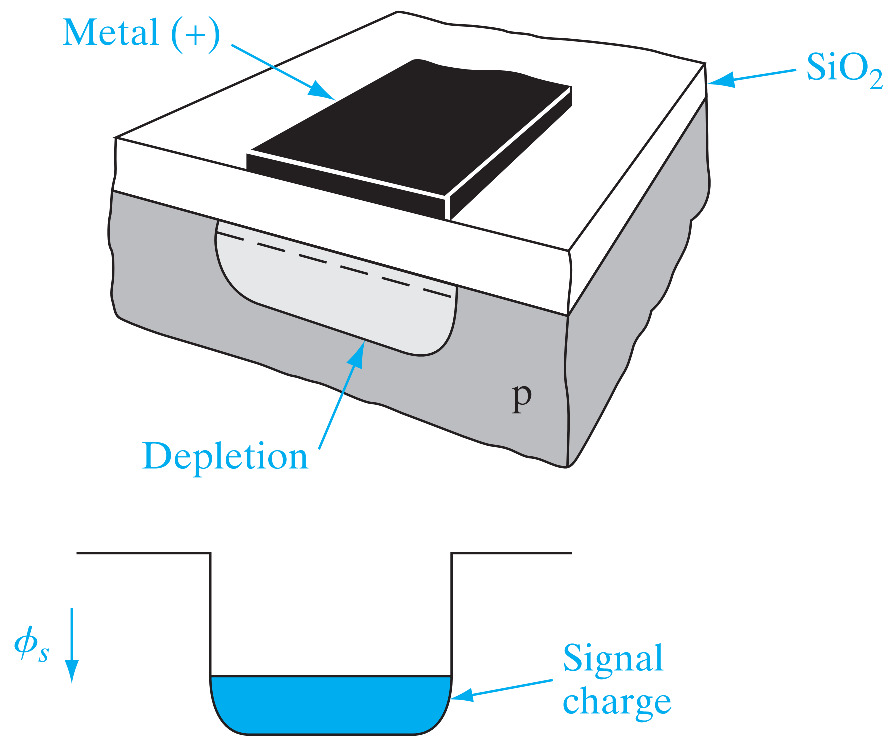

Figure 9–15
An MOS capacitor with a positive gate pulse: (a) depletion region and surface charge; (b) potential well at the interface, partially filled with electrons corresponding to the surface charge shown in (a).

[3]The potential well should not be confused with the depletion region, which extends into the bulk of the semiconductor. The "depth" of the well is measured in electrostatic potential, not distance. Electrons stored in the potential well are in fact located very near the semiconductor surface.

From: Solid State Electronic Devices by Ben Streetman, Sanjay Banerjee

CCD Readout

Figure 9–16
The basic CCD, composed of a linear array of MOS capacitors. At time t_1, the G_1 electrodes are positive, and the charge packet is stored in the G_1 potential well. At t_2 both G_1 and G_2 are positive, and the charge is distributed between the two wells. At t_3 the potential on G_1 is reduced, and the charge flows to the second well. At t_4 the transfer of charge to the G_2 well is completed.

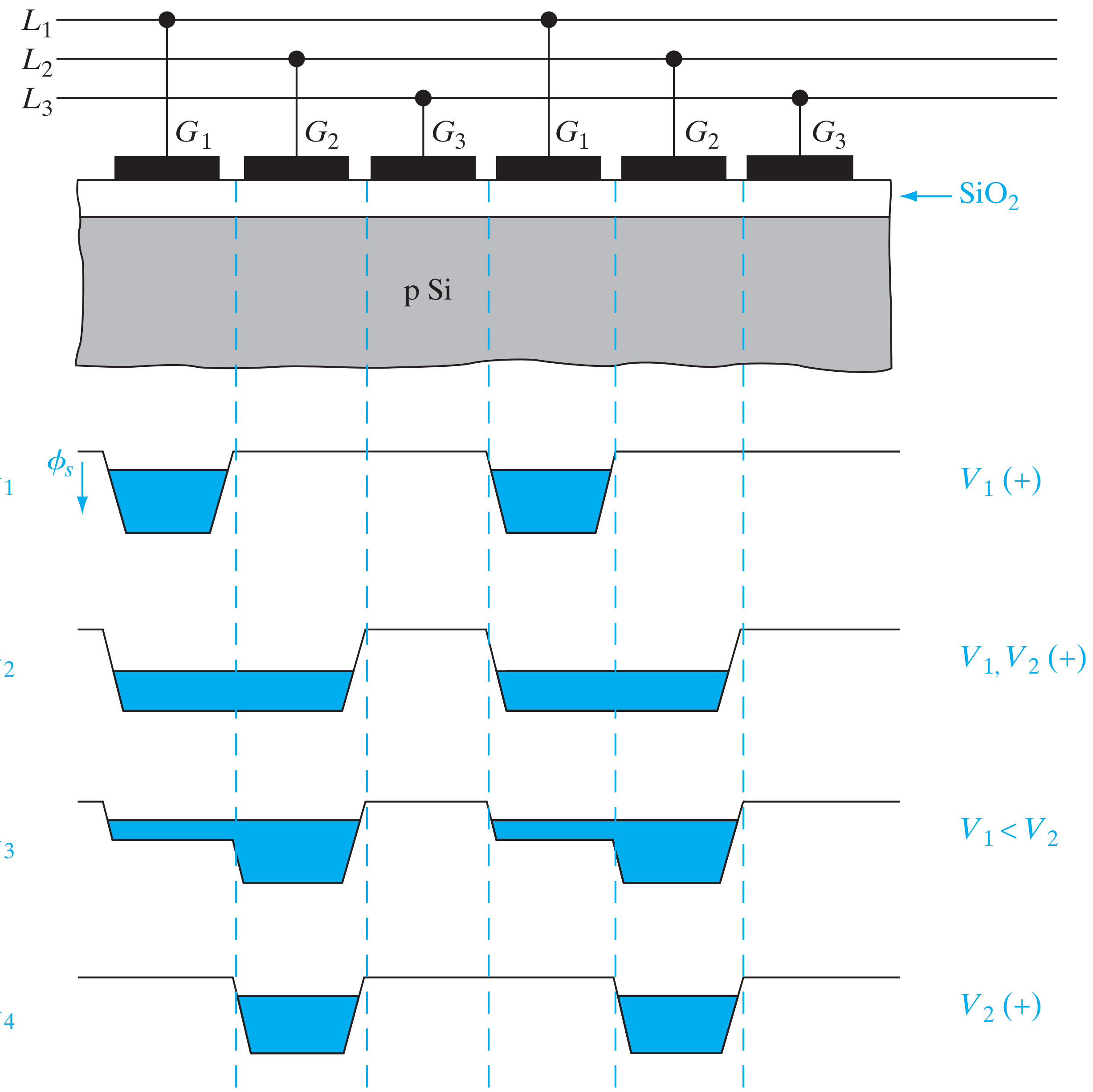

From: Solid State Electronic Devices by Ben Streetman, Sanjay Banerjee

CCD Readout

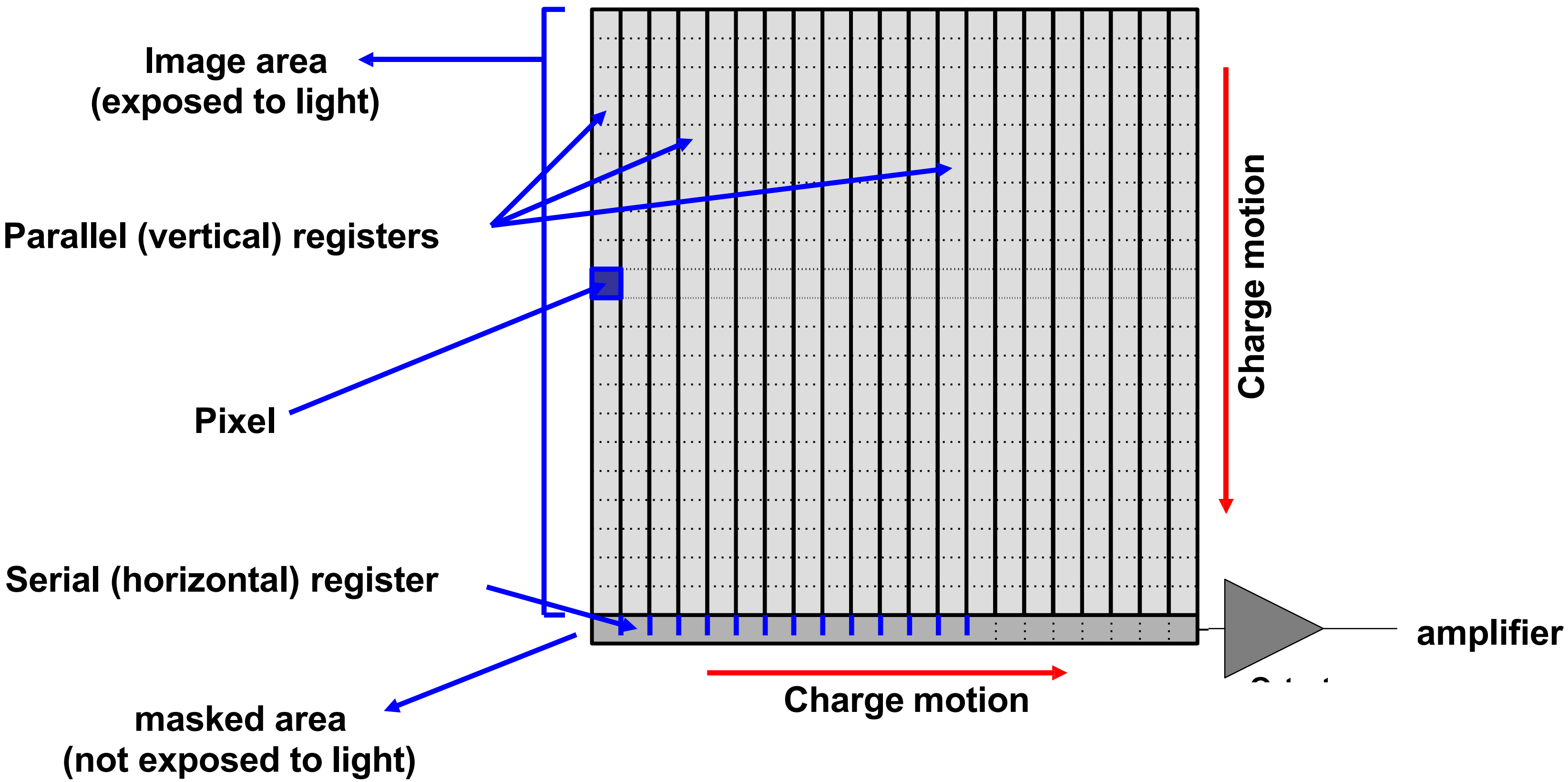

- Shift register
- Destructive measurement of charge in the amplifier
- Scientific CCD reach 2e^{-} RMS

Skipper CCD

"Skipper CCD is the most sensitive and robust electromagnetic calorimeter that can operate above liquid nitrogen temperatures."

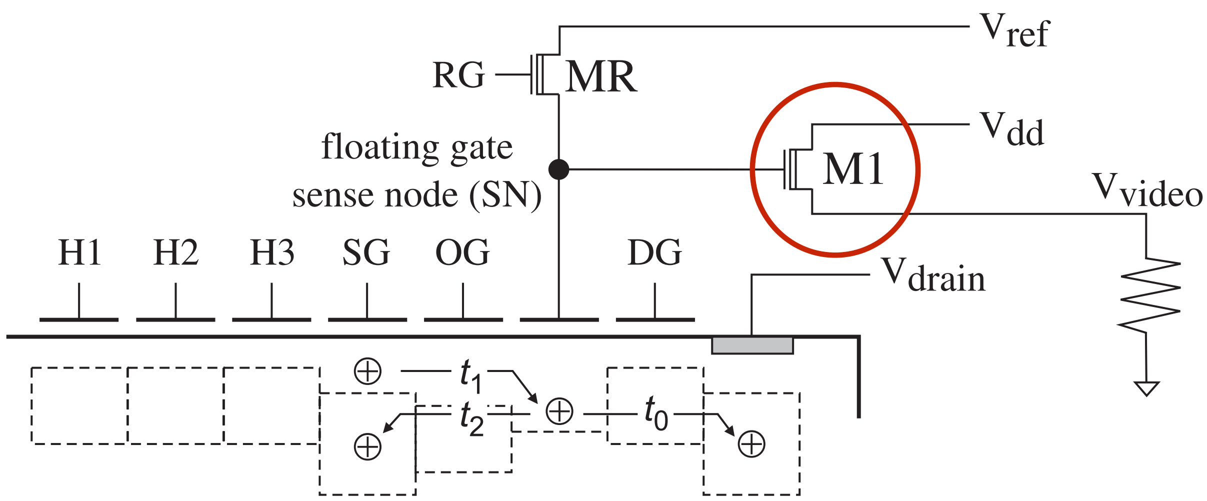

FIG. 2. Schematic of the Skipper CCD output stage. H1, H2, and H3 are the horizontal register clock phases. MR is a switch to reset the sense node to V_{ref}. M1 is a MOSFET in a source follower configuration. Because of its floating gate, the Skipper CCD readout performs a nondestructive measurement of the charge at the SN.

- Non-Destructive measurement of charge, allows multiple sampling

Tiffenberg et al, PRL 119, 131802 (2017)

Skipper CCD Multiple sampling

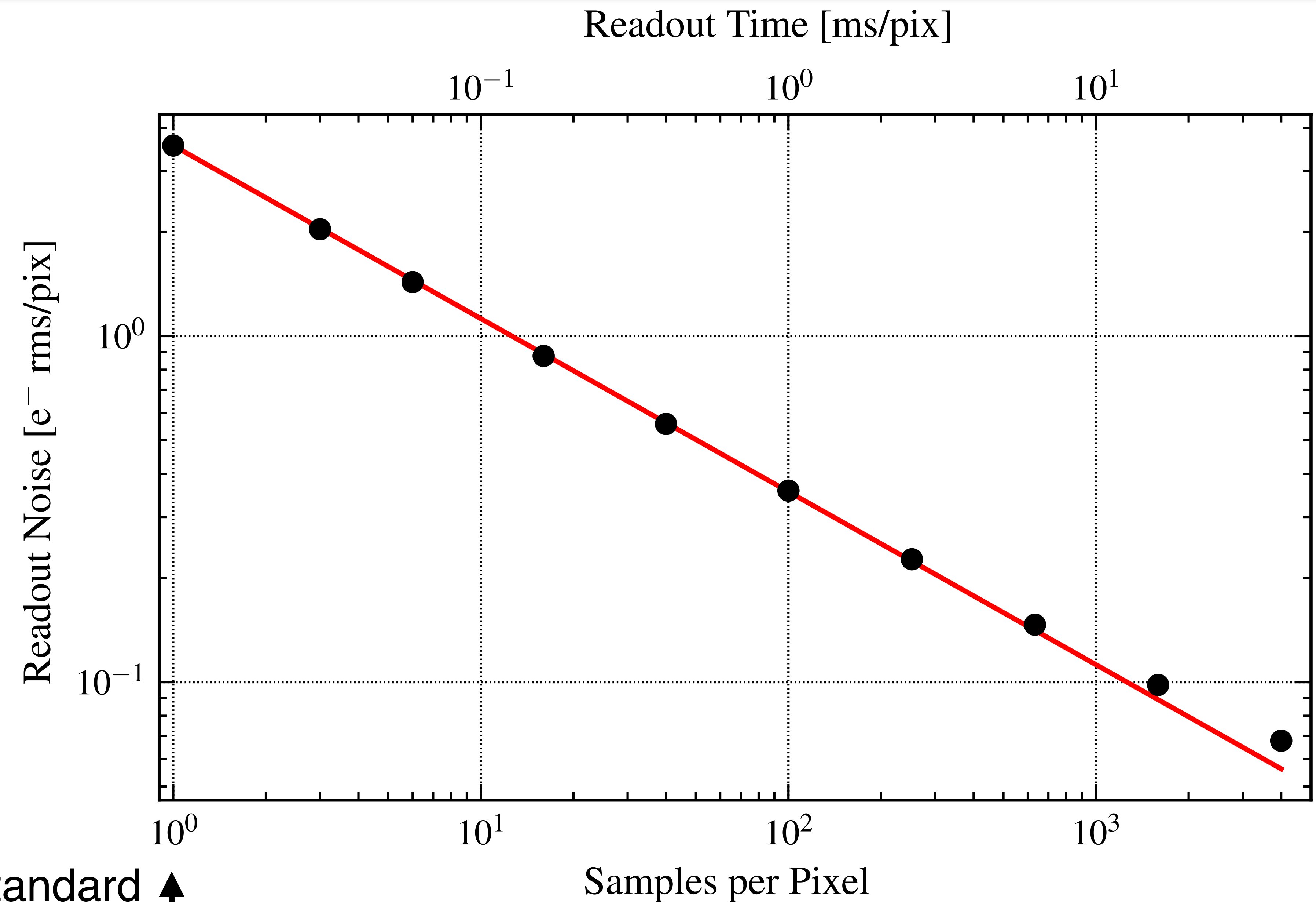

Standard CCD ↑

CCD as particle detector

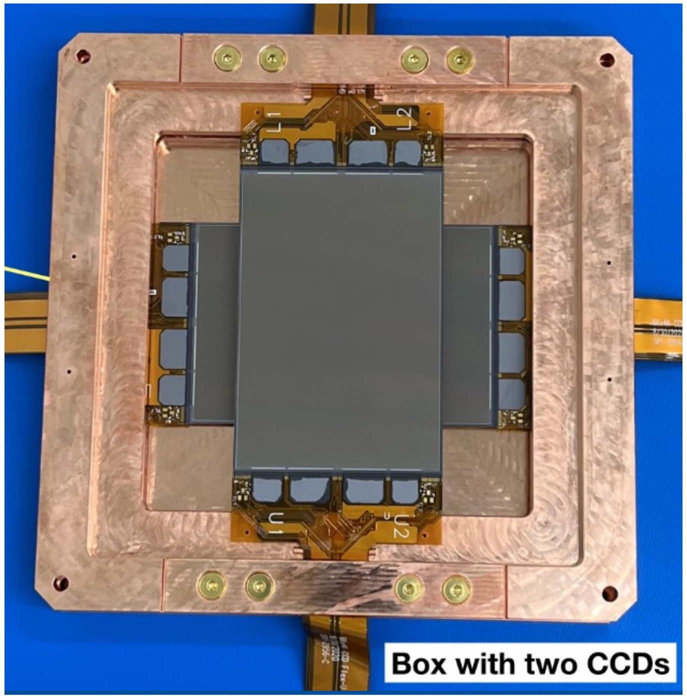

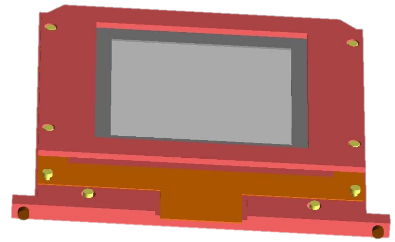

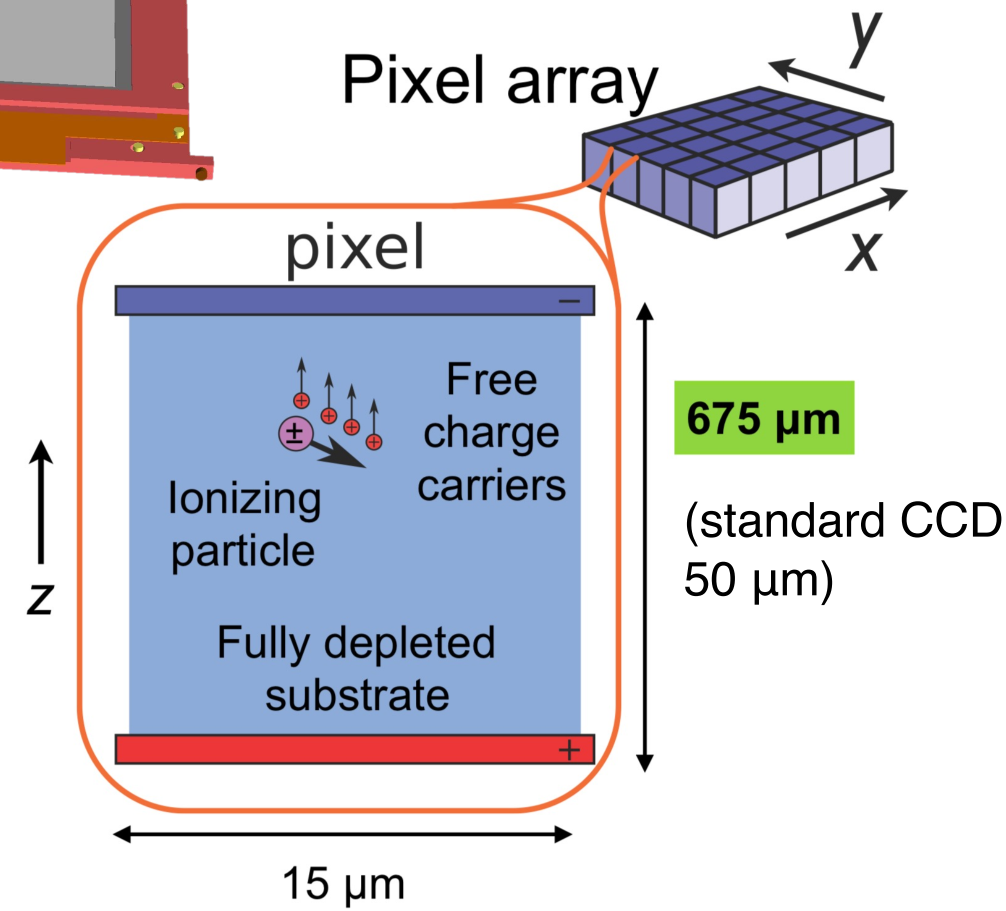

- Pros: low dark rates, few eV threshold, 10 micron position resolution,
- Cons: silicon target only, lack of timing, no discrimination

CCD - Data

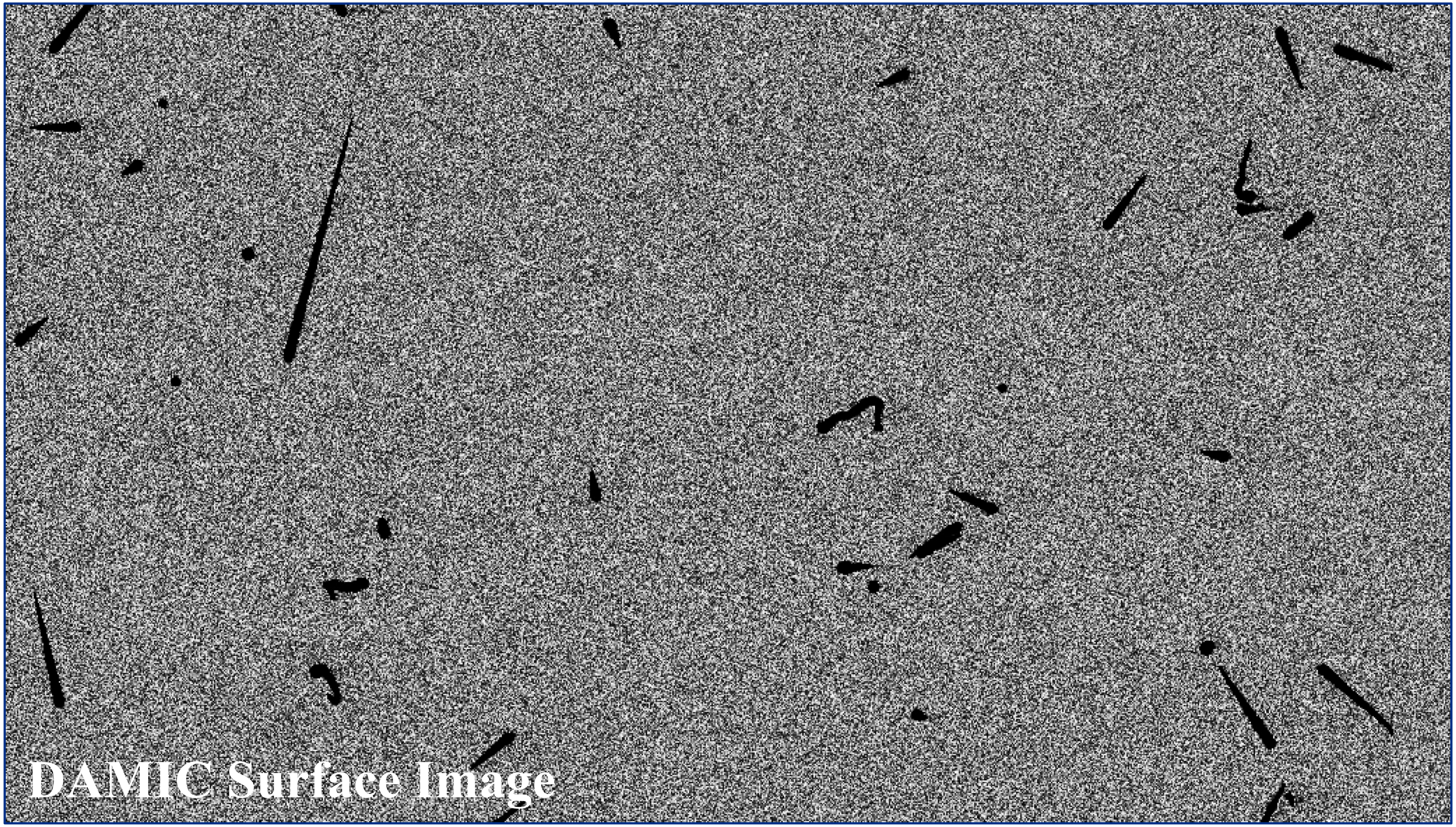

CCD - Data

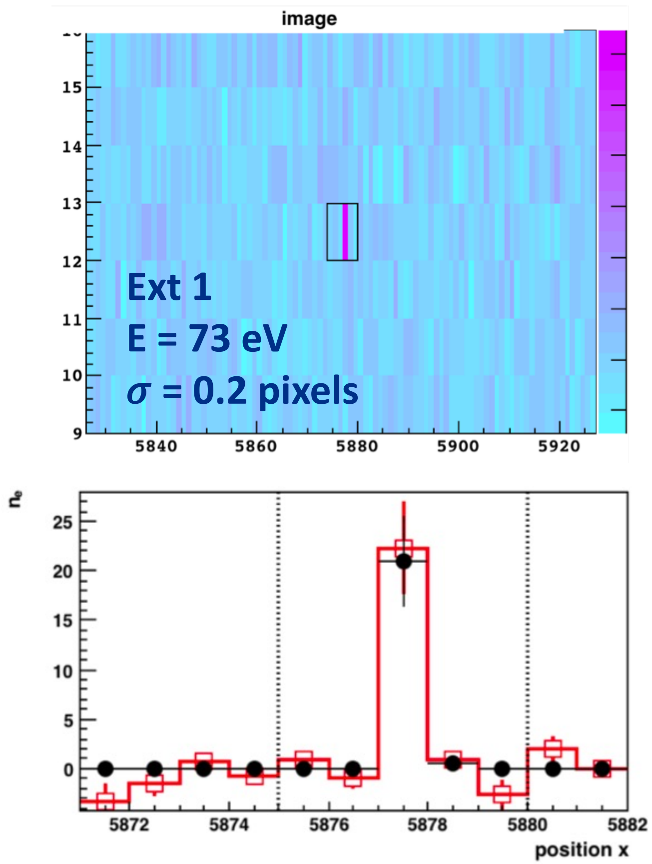
image
Ext 1
E = 73 eV
σ = 0.2 pixels
5840 5860 5880 5900 5920
n_e
5872 5874 5876 5878 5880 5882
position x

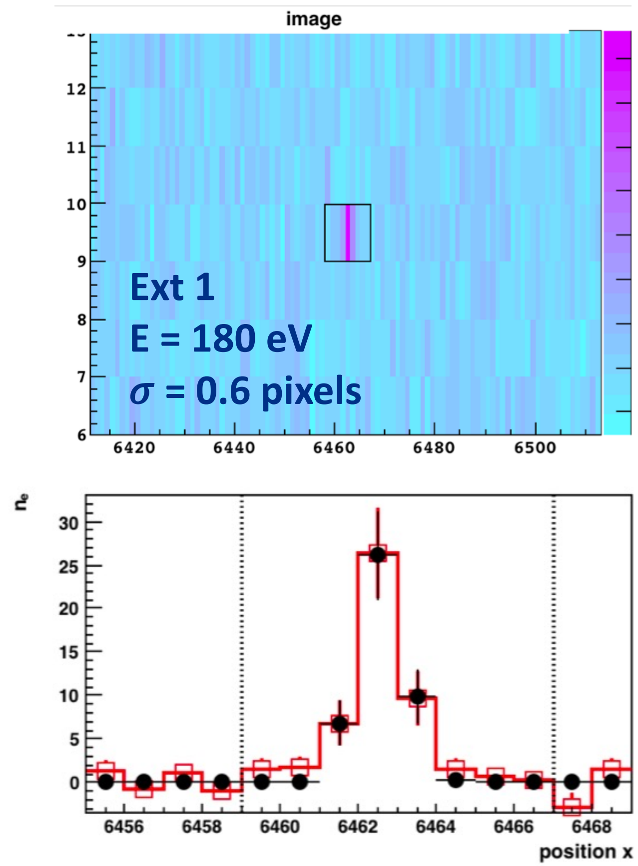
image
Ext 1
E = 180 eV
σ = 0.6 pixels
6420 6440 6460 6480 6500
n_e
6456 6458 6460 6462 6464 6466 6468
position x

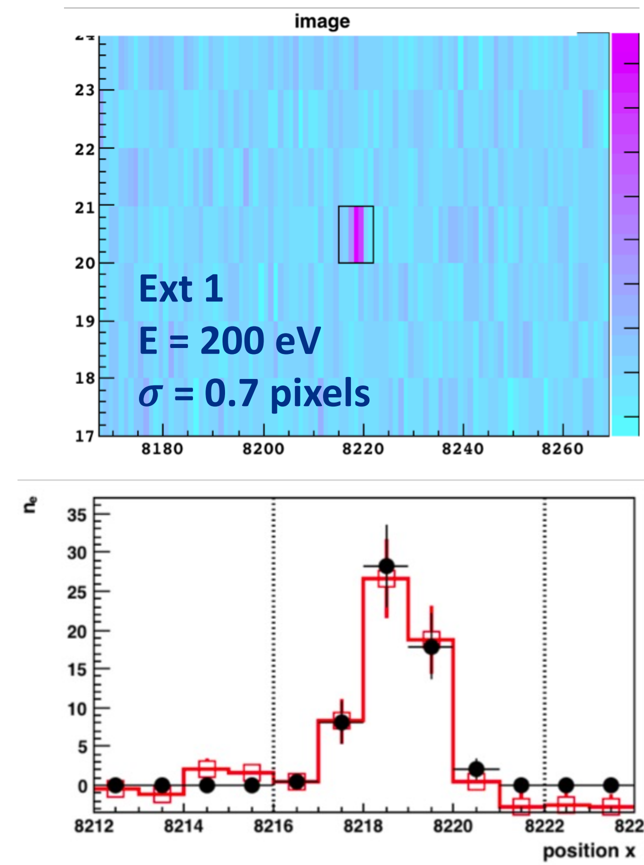
image
Ext 1
E = 200 eV
σ = 0.7 pixels
8180 8200 8220 8240 8260
n_e
8212 8214 8216 8218 8220 8222 8224
position x

DAMIC-M at Modane

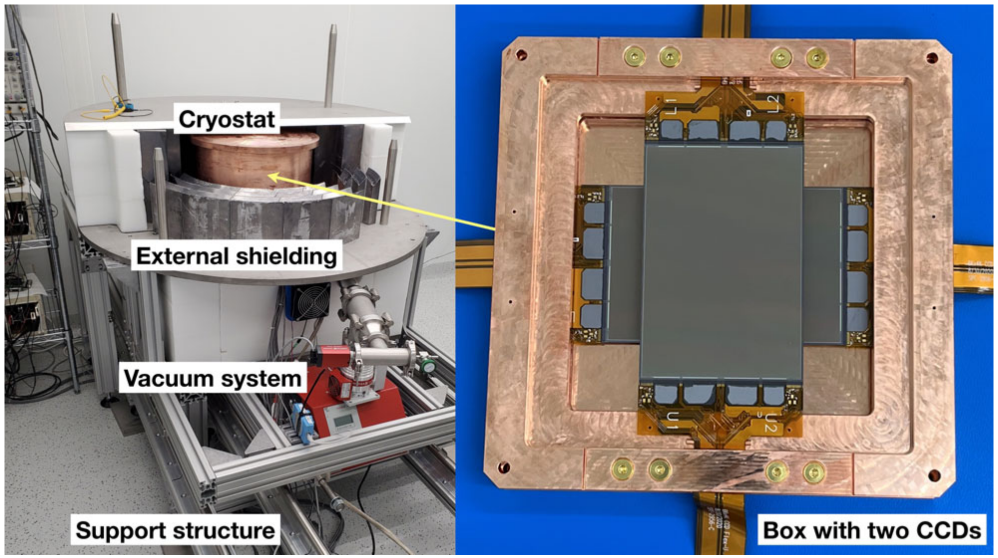

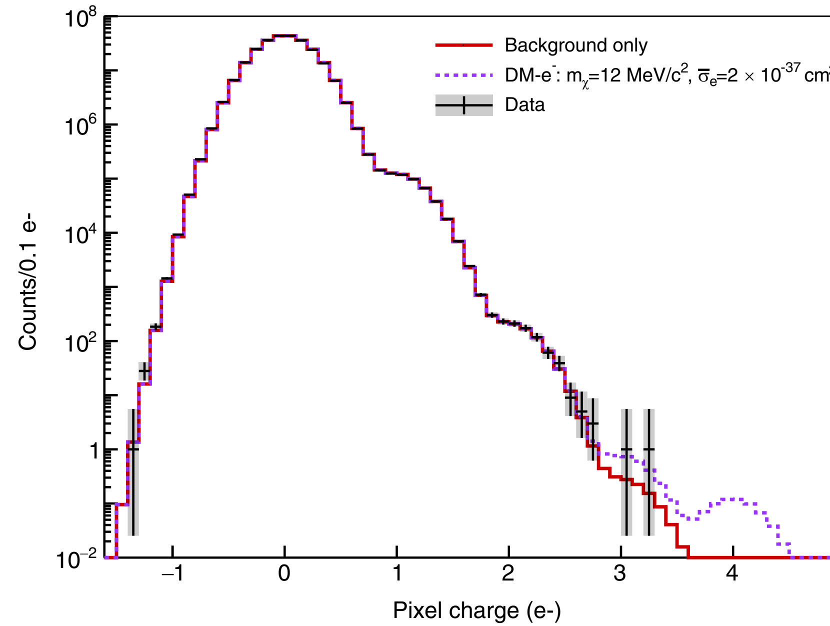

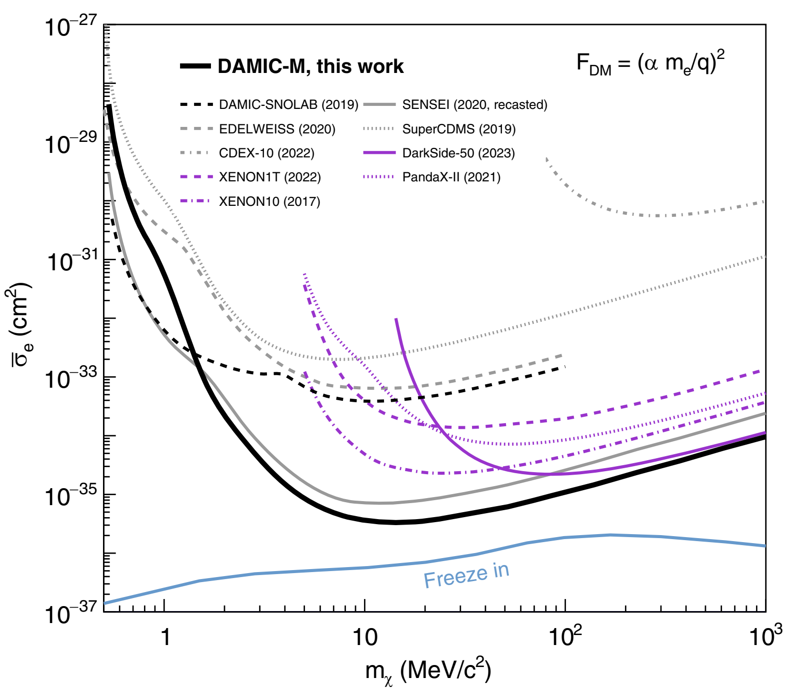

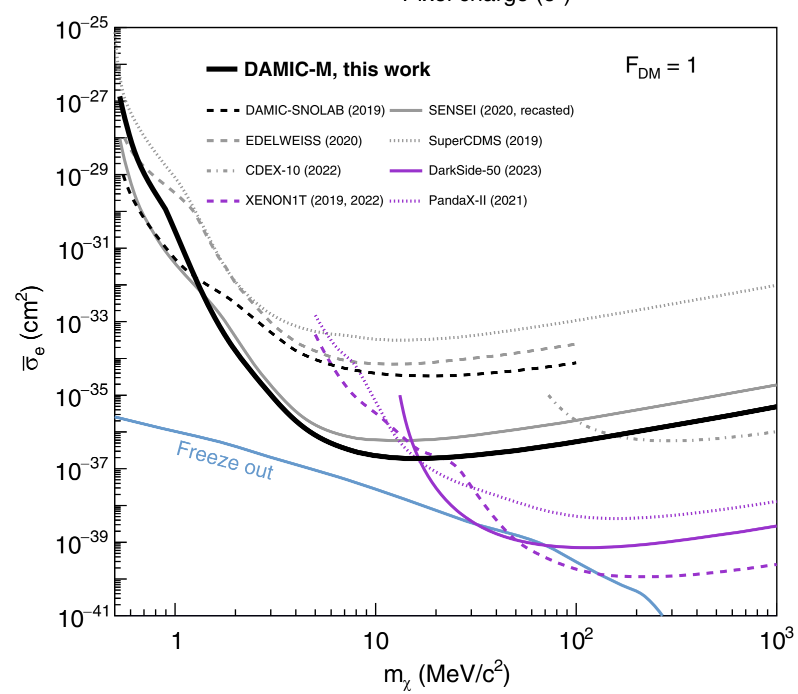

Crystals

Scintillation

- Presence in the forbidden band of states due to impurities (natural or doped)
- Electrons excited by interacting particles can populate this states and later decay emitting photons
- The crystal is transparent to this photons

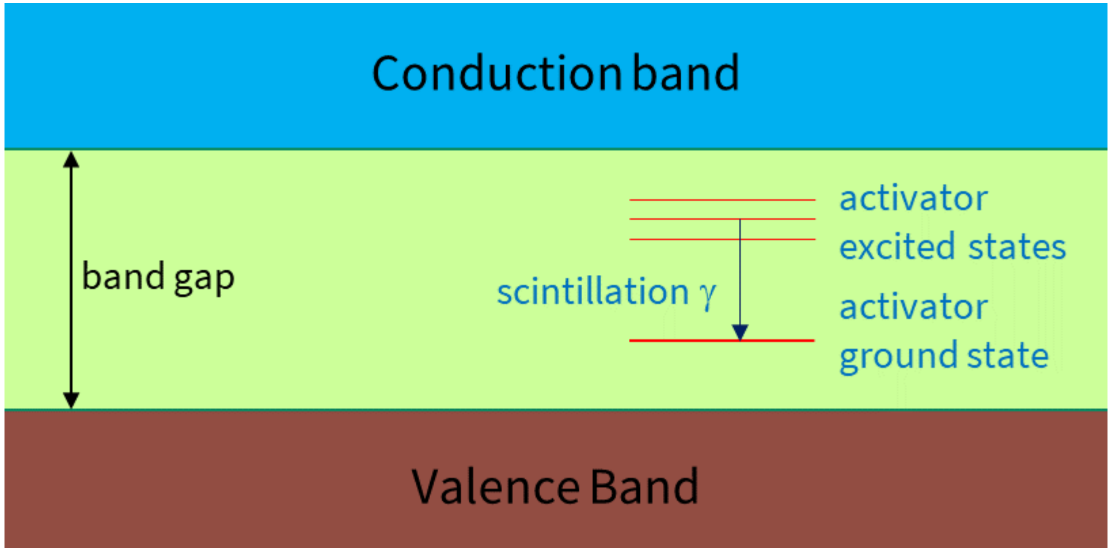

Scintillation

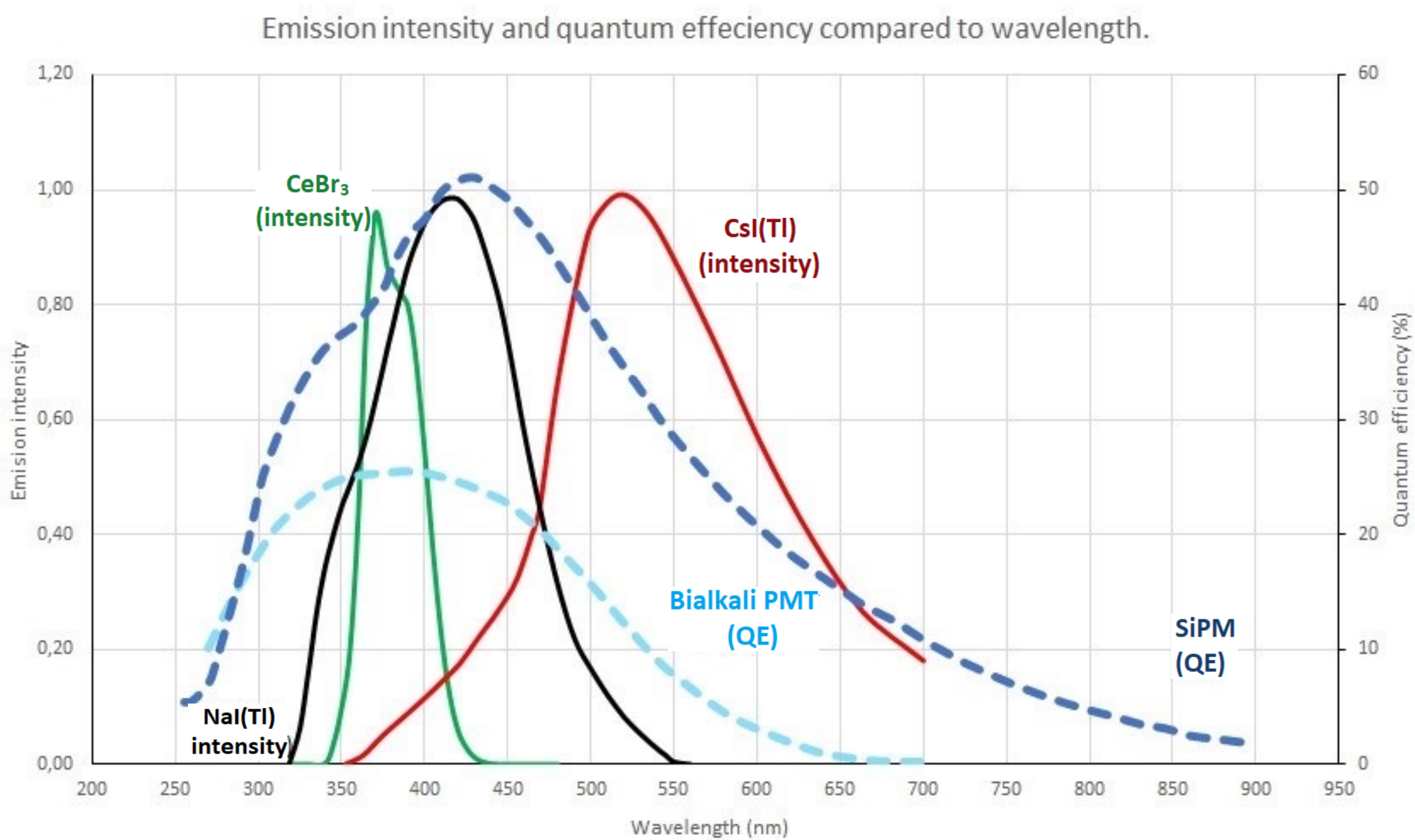

Common scintillators

Table 8.3 Properties of Common Inorganic Scintillators

	Specific Gravity	Wavelength of Max. Emission	Refractive Index	Decay Time (μs)	Abs. Light Yield in Photons/MeV	Relative Pulse Height Using Bialk. PM tube	References
Alkali Halides							
NaI(Tl)	3.67	415	1.85	0.23	38 000	1.00	
CsI(Tl)	4.51	540	1.80	0.68 (64%), 3.34 (36%)	65 000	0.49	78, 90, 91
CsI(Na)	4.51	420	1.84	0.46, 4.18	39 000	1.10	92
Li(Eu)	4.08	470	1.96	1.4	11 000	0.23	
Other Slow Inorganics							
BGO	7.13	480	2.15	0.30	8200	0.13	
$CdWO_4$	7.90	470	2.3	1.1 (40%), 14.5 (60%)	15 000	0.4	98–100
ZnS(Ag) (polycrystalline)	4.09	450	2.36	0.2		1.3[a]	
CaF_2 (Eu)	3.19	435	1.47	0.9	24 000	0.5	
Unactivated Fast Inorganics							
BaF_2 (fast component)	4.89	220		0.0006	1400	na	107–109
BaF_2 (slow component)	4.89	310	1.56	0.63	9500	0.2	107–109
CsI (fast component)	4.51	305		0.002 (35%), 0.02 (65%)	2000	0.05	113–115
CsI (slow component)	4.51	450	1.80	multiple, up to several μs	varies	varies	114, 115
CeF_3	6.16	310, 340	1.68	0.005, 0.027	4400	0.04 to 0.05	76, 116, 117
Cerium-Activated Fast Inorganics							
GSO	6.71	440	1.85	0.056 (90%), 0.4 (10%)	9000	0.2	119–121
YAP	5.37	370	1.95	0.027	18 000	0.45	78, 125
YAG	4.56	550	1.82	0.088 (72%), 0.302 (28%)	17 000	0.5	78, 127
LSO	7.4	420	1.82	0.047	25 000	0.75	130, 131
LuAP	8.4	365	1.94	0.017	17 000	0.3	134, 136, 138
Glass Scintillators							
Ce activated Li glass[b]	2.64	400	1.59	0.05 to 0.1	3500	0.09	77, 145
Tb activated glass[b]	3.03	550	1.5	~3000 to 5000	~50 000	na	145
For comparison, a typical organic (plastic) scintillator:							
NE102A	1.03	423	1.58	0.002	10 000	0.25	

[a]for alpha particles

[b]Properties vary with exact formulation. Also see Table 15.1.

Source: Data primarily from Refs. 74 and 75, except where noted.

from «Radiation detection and measurement», G.F. Knoll

Light readout

Detectors:

- Photomultiplers (PMT)
- Avalanche Photodiode (APD)
- Silicon Photomultipliers (SiPM)

Transmission to sensors: light guide

- Note that the light guide is not a funnel!

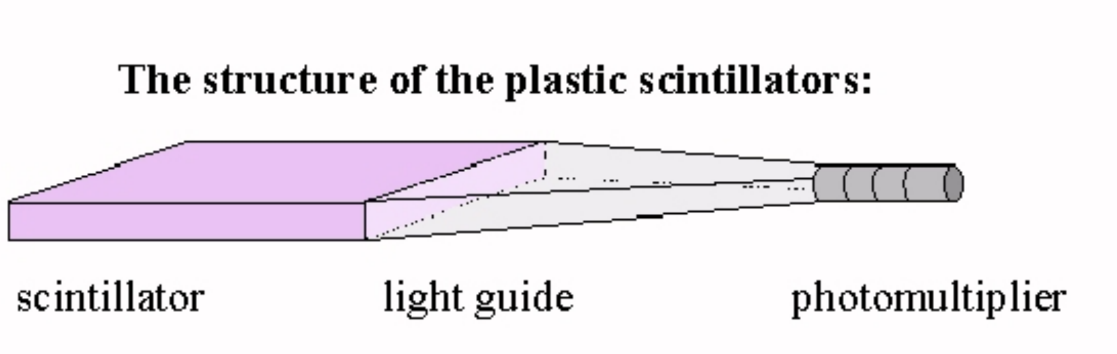

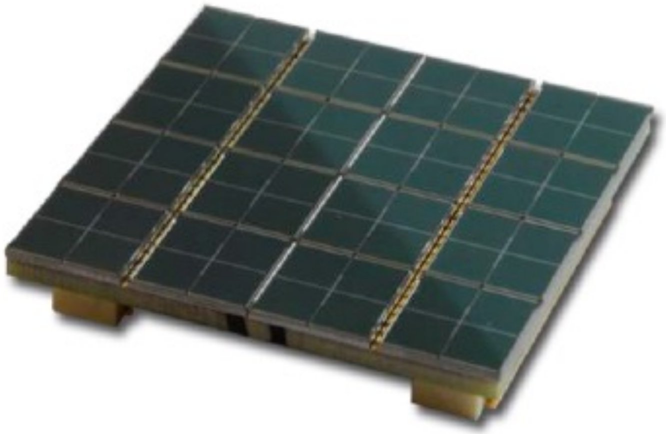

DAMA/LIBRA

- 25 NaI crystals, 9.70 kg each
- High radiopurity: ^{232}Th and ^{238}U (ppt), ^{40}K (<20 ppb)

  Dual read-out of each crystal via PMTs (noise reduction via coincidence), 5.5-7.5 photoelectrons/keVee
- Energy threshold: 1 keVee
- Granularity: select single crystal events

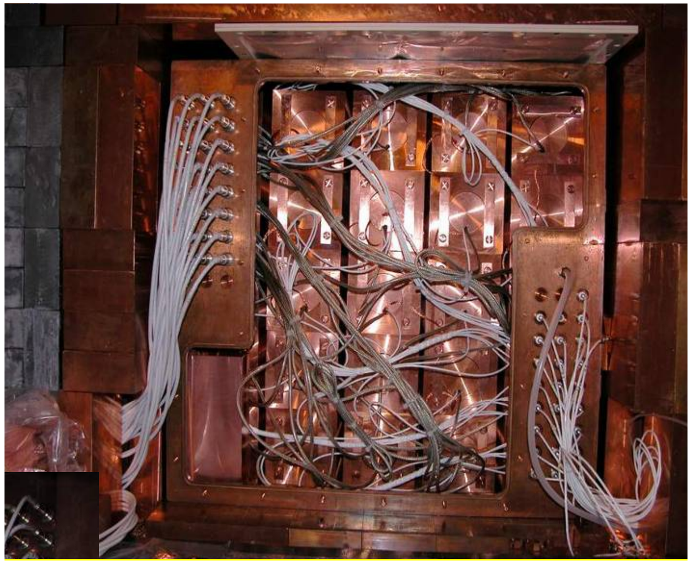

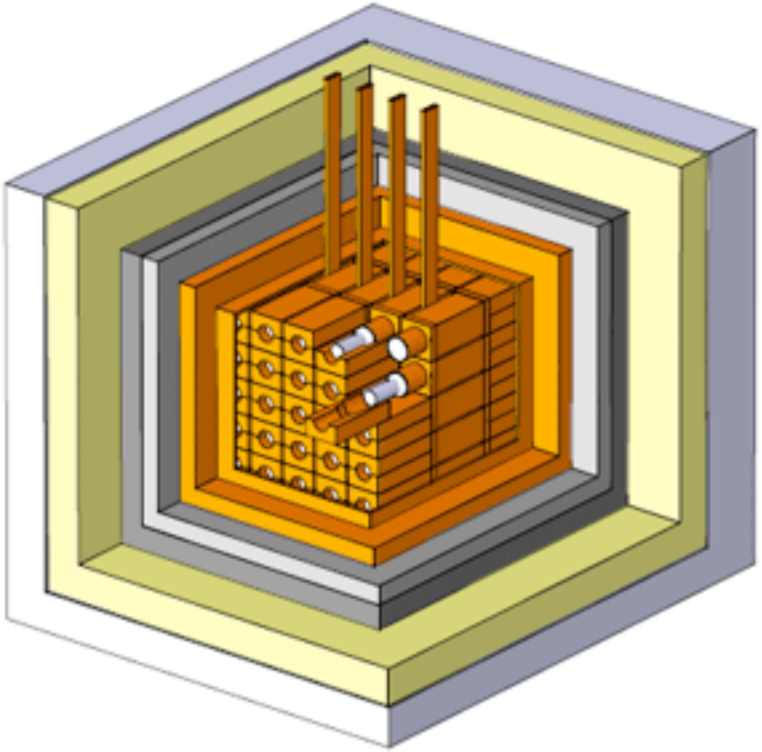

DAMA/LIBRA - data analysis

Pulse shape cuts to reject PMT noise events:

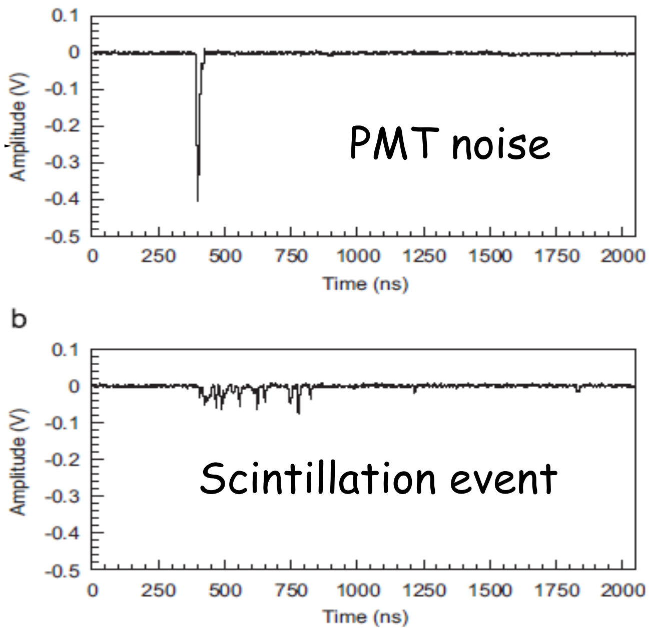

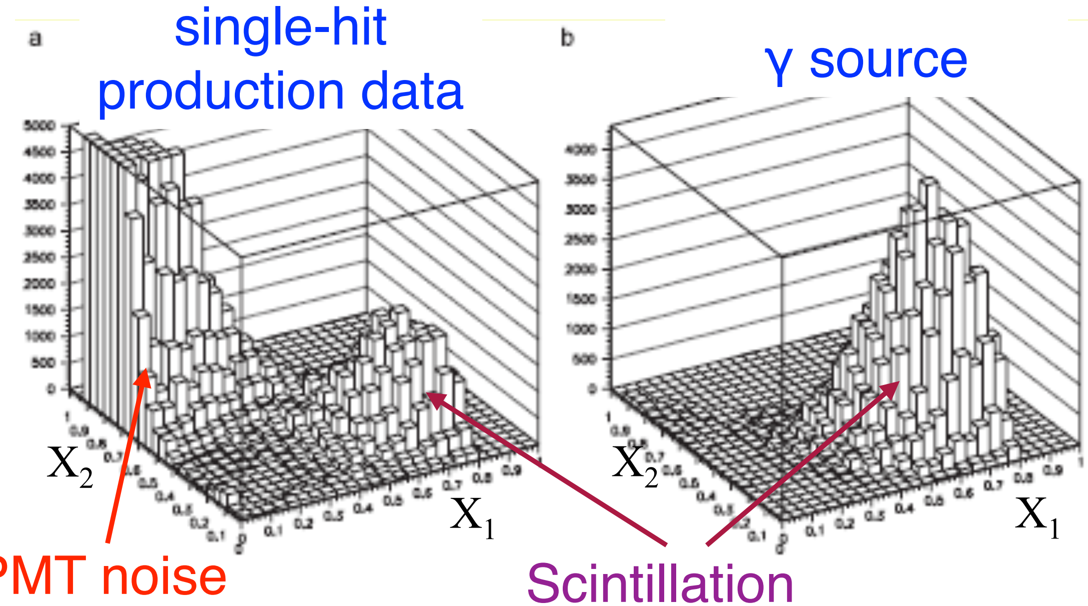

Low energy calibration with ^{241}Am and ^{133}Ba, check with ^{40}K

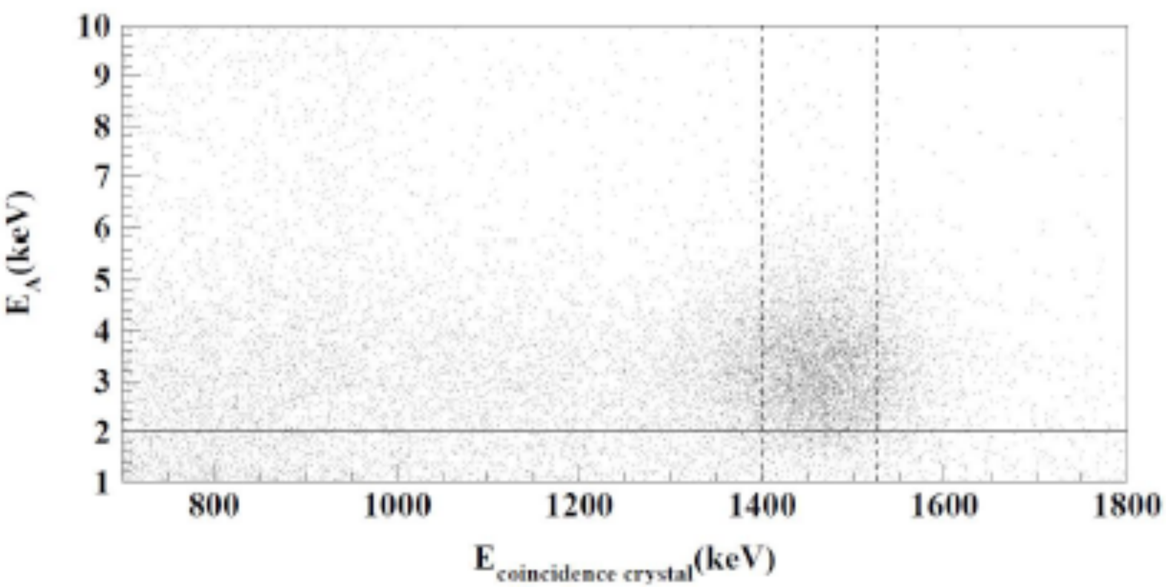

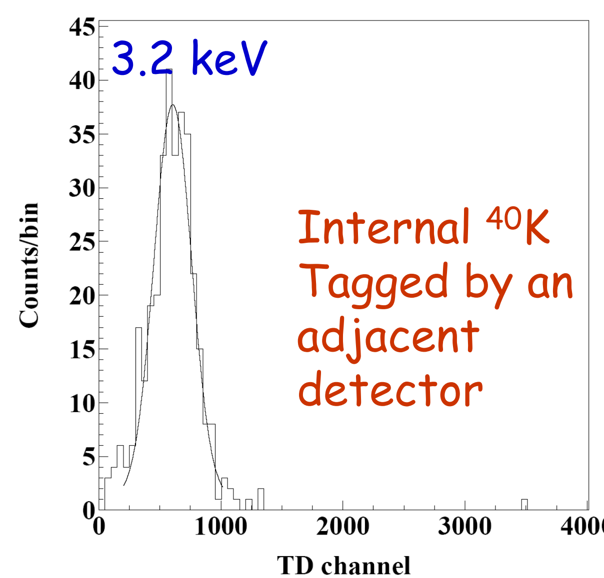

Counting rate annual modulation

Earth velocity combines to solar system velocity in the galaxy.

Dark matter "wind" in the heart rest frame is modulated:

$$v(t) = v_{\text{sun}} + v_{\text{orb}}^{||} \cos[\omega(t - t_0)]$$

and affects the counting rate:

$$S(E,t) = S_0(E) + S_m(E) \cos[\omega(t - t_0)]$$

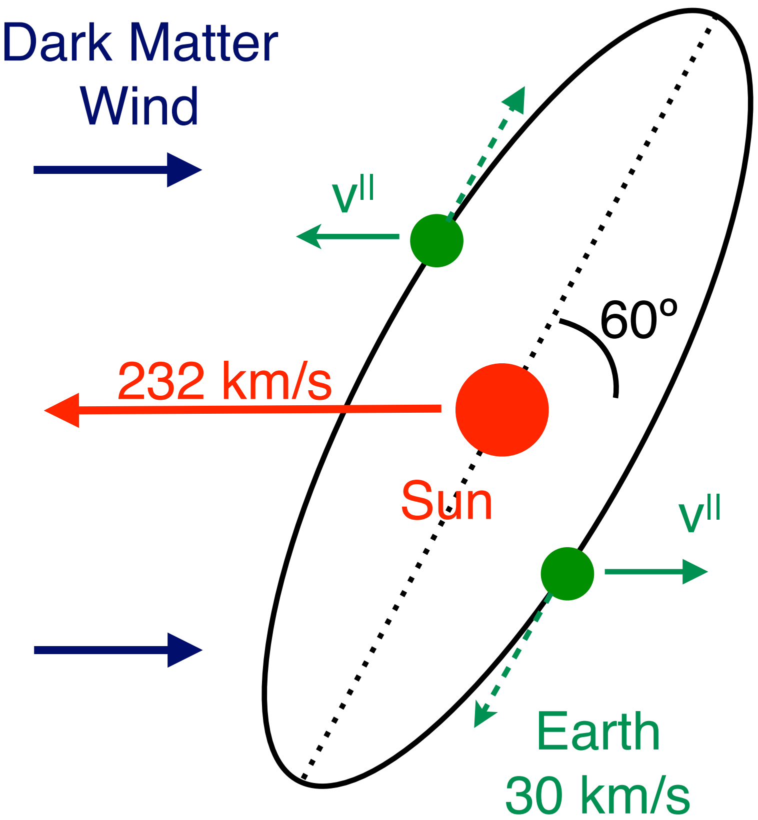

Distinctive modulation signal features:

T = 1 year t_0 = 2nd June

Pro: model independent   **Con:** requires detector stability and bkg control.

Modulation spectrum

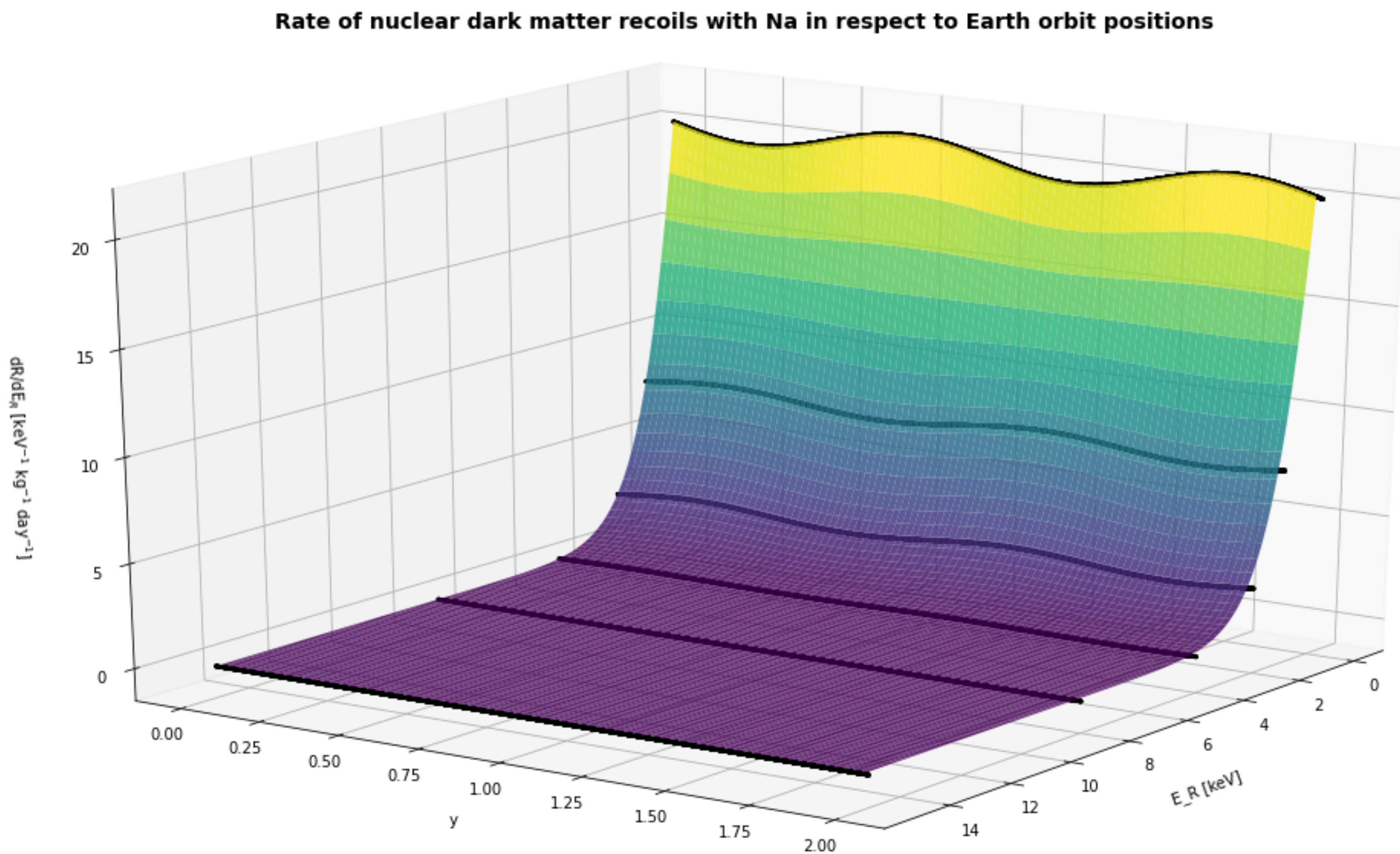

Davide Marin, Student of Neutrinos and Dark Matter at Sapienza

DAMA/LIBRA results

ЯДЕРНА ФІЗИКА ТА ЕНЕРГЕТИКА / NUCL. PHYS. AT. ENERGY 19 (2018) 307-325 ISSN 1818-331X

ЯДЕРНА ФІЗИКА
NUCLEAR PHYSICS

УДК 539.1.074.3, 524.8 https://doi.org/10.15407/jnpae2018.04.307

R. Bernabei[1,2,*], P. Belli[1,2], A. Bussolotti[2], F. Cappella[3,4], V. Caracciolo[5], R. Cerulli[1,2], C. J. Dai[6], A. d'Angelo[3,4], A. Di Marco[2], H. L. He[6], A. Incicchitti[3,4], X. H. Ma[6], A. Mattei[4], V. Merlo[1,2], F. Montecchia[2,7], X. D. Sheng[6], Z. P. Ye[6,8]

[1] Dipartimento di Fisica, Università di Roma "Tor Vergata", Rome, Italy
[2] INFN, sez. Roma "Tor Vergata", Rome, Italy
[3] Dipartimento di Fisica, Università di Roma "La Sapienza", Rome, Italy
[4] INFN, Sezione di Roma, Rome, Italy
[5] INFN Laboratori Nazionali del Gran Sasso, Assergi, Italy
[6] Key Laboratory of Particle Astrophysics, Institute of High Energy Physics, Chinese Academy of Sciences, Beijing, P.R. China
[7] Dipartimento Ingegneria Civile e Ingegneria Informatica, Università di Roma "Tor Vergata", Rome, Italy
[8] University of Jinggangshan, Ji'an, Jiangxi, P.R. China

*Corresponding author: rita.bernabei@roma2.infn.it

FIRST MODEL INDEPENDENT RESULTS FROM DAMA/LIBRA-PHASE2

The first model independent results obtained by the DAMA/LIBRA-phase2 experiment are presented. The data have been collected over 6 annual cycles corresponding to a total exposure of 1.13 t · yr, deep underground at the Gran Sasso National Laboratory (LNGS) of the I.N.F.N. The DAMA/LIBRA-phase2 apparatus, $\simeq$ 250 kg highly radio-pure NaI(Tl), profits from a second generation high quantum efficiency photomultipliers and of new electronics with respect to DAMA/LIBRA-phase1. The improved experimental configuration has also allowed to lower the software energy threshold. New data analysis strategies are presented. The DAMA/LIBRA-phase2 data confirm the evidence of a signal that meets all the requirements of the model independent Dark Matter (DM) annual modulation signature, at 9.5 σ C.L. in the energy region (1 - 6) keV. In the energy region between 2 and 6 keV, where data are also available from DAMA/NaI and DAMA/LIBRA-phase1 (exposure 1.33 t · yr, collected over 14 annual cycles), the achieved C.L. for the full exposure (2.46 t · yr) is 12.9 σ; the modulation amplitude of the *single-hit* scintillation events is: (0.0103 ± ± 0.0008) cpd/kg/keV, the measured phase is (145 ± 5) d and the measured period is (0.999 ± 0.001) yr, all these values are well in agreement with those expected for DM particles. No systematics or side reaction able to mimic the exploited DM signature (i.e. to account for the whole measured modulation amplitude and to simultaneously satisfy all the requirements of the signature), has been found or suggested by anyone throughout some decades thus far.

Keywords: scintillation detectors, elementary particle processes, Dark Matter.
PACS numbers: 29.40.Mc; 95.30.Cq; 95.35.+d.

Dama/LIBRA results

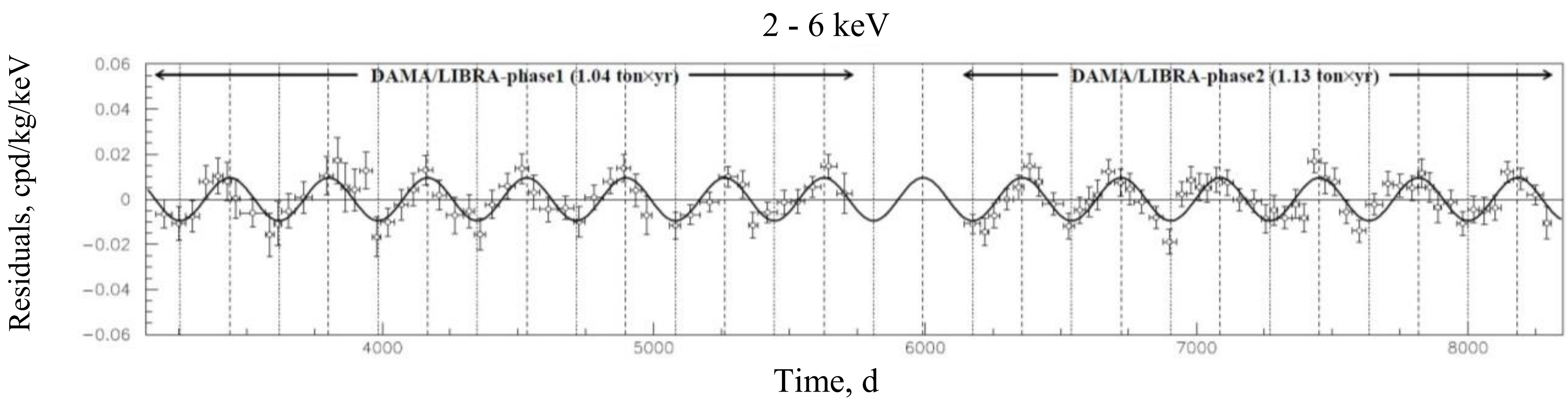

Fig. 3. Experimental residual rate of the *single-hit* scintillation events measured by DAMA/LIBRA-phase1 and DAMA/LIBRA-phase2 in the (2 - 6) keV energy intervals as a function of the time. The superimposed curve is the cosinusoidal functional forms $A \cos \omega(t - t_0)$ with a period $T = 2\pi/\omega = 1$ yr, a phase t_0 = 152.5 d (June 2nd) and modulation amplitude, A, equal to the central value obtained by best fit on the data points of DAMA/LIBRA-phase1 and DAMA/LIBRA-phase2. For details see Fig. 2.

DAMA: Modulation amplitude

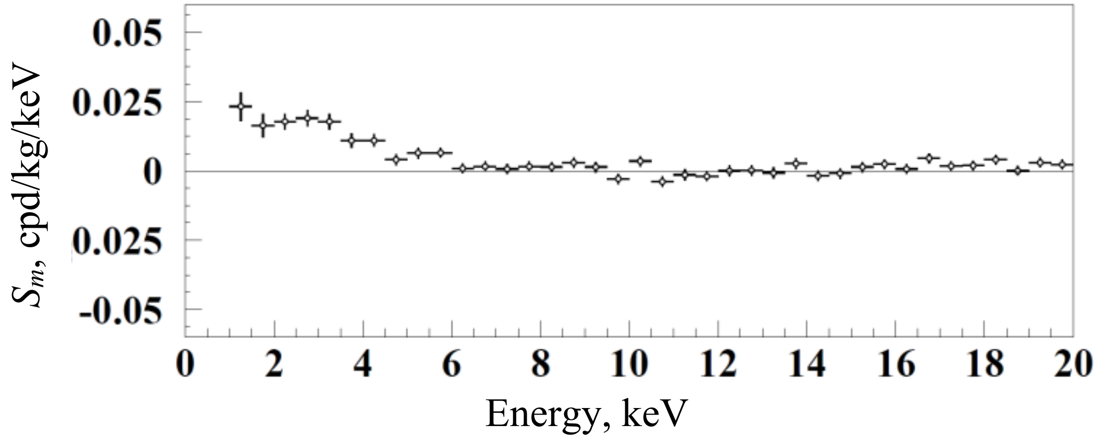

Fig. 11. Modulation amplitudes, S_m, for the whole data sets: DAMA/NaI, DAMA/LIBRA-phase1 and DAMA/LIBRA-phase2 (total exposure 2.46 t · yr) above 2 keV; below 2 keV only the DAMA/LIBRA-phase2 exposure (1.13 t · yr) is available and used. The energy bin ΔE is 0.5 keV. A clear modulation is present in the lowest energy region, while S_m values compatible with zero are present just above. In fact, the S_m values in the (6 - 20) keV energy interval have random fluctuations around zero with χ^2 equal to 42.6 for 28 *d.o.f.* (upper tail probability of 4 %).

DAMA/LIBRA - checks

R. Cerulli at IDM2012

Source	Main comment	Cautious upper limit (90%C.L.)
RADON	Sealed Cu box in HP Nitrogen atmosphere, 3-level of sealing, etc.	**$<2.5\times10^{-6}$ cpd/kg/keV**
TEMPERATURE	Installation is air conditioned+ detectors in Cu housings directly in contact with multi-ton shield→ huge heat capacity + T continuously recorded	**$<10^{-4}$ cpd/kg/keV**
NOISE	Effective full noise rejection near threshold	**$<10^{-4}$ cpd/kg/keV**
ENERGY SCALE	Routine + intrinsic calibrations	**$<1\text{-}2\times10^{-4}$ cpd/kg/keV**
EFFICIENCIES	Regularly measured by dedicated calibrations	**$<10^{-4}$ cpd/kg/keV**
BACKGROUND	No modulation above 6 keV; no modulation in the (2-6) keV *multiple-hits* events; this limit includes all possible sources of background	**$<10^{-4}$ cpd/kg/keV**
SIDE REACTIONS	Muon flux variation measured at LNGS	**$<3\times10^{-5}$ cpd/kg/keV**

+ they cannot satisfy all the requirements of annual modulation signature

Thus, they cannot mimic the observed annual modulation effect

DAMA phase: May 26±7 μ phase @LNGS: July 6±6

Constraint from COSINE

Three-year annual modulation search with COSINE-100

G. Adhikari,[1] E. Barbosa de Souza,[2] N. Carlin,[3] J. J. Choi,[4] S. Choi,[4] A. C. Ezeribe,[5] L. E. França,[3] C. Ha,[6] I. S. Hahn,[7,8,9] S. J. Hollick,[2] E. J. Jeon,[10] J. H. Jo,[2] H. W. Joo,[4] W. G. Kang,[10] M. Kauer,[11] H. Kim,[10] H. J. Kim,[12] J. Kim,[6] K. W. Kim,[10] S. H. Kim,[10] S. K. Kim,[4] W. K. Kim,[9,10] Y. D. Kim,[10,13,9] Y. H. Kim,[10,14,9] Y. J. Ko,[10] H. J. Kwon,[9,10] D. H. Lee,[12] E. K. Lee,[10] H. Lee,[9,10] H. S. Lee,[10,9] H. Y. Lee,[10] I. S. Lee,[10] J. Lee,[10] J. Y. Lee,[12] M. H. Lee,[10,9] S. H. Lee,[9,10] S. M. Lee,[4] D. S. Leonard,[10] B. B. Manzato,[3] R. H. Maruyama,[2] R. J. Neal,[5] B. J. Park,[9,10] H. K. Park,[15] H. S. Park,[14] K. S. Park,[10] S. D. Park,[12] R. L. C. Pitta,[3] H. Prihtiadi,[10] S. J. Ra,[10] C. Rott,[16,17] K. A. Shin,[10] A. Scarff,[5] N. J. C. Spooner,[5] W. G. Thompson,[2,*] L. Yang,[1] and G. H. Yu[16]

(COSINE-100 Collaboration)

COSINE-100 is a direct detection dark matter experiment that aims to test DAMA/LIBRA's claim of dark matter discovery by searching for a dark-matter-induced annual modulation signal with NaI(Tl) detectors. We present new constraints on the annual modulation signal from a dataset with a 2.82 yr livetime utilizing an active mass of 61.3 kg for a total exposure of 173 kg · yr. This new result features an improved event selection that allows for both lowering the energy threshold to 1 keV and a more precise time-dependent background model. In the 1–6 and 2–6 keV energy intervals, we observe best-fit values for the modulation amplitude of 0.0067 ± 0.0042 and 0.0051 ± 0.0047 counts/(day · kg · keV), respectively, with a phase fixed at 152.5 days.

G. ADHIKARI et al.
PHYS. REV. D 106, 052005 (2022)

COSINE - Results

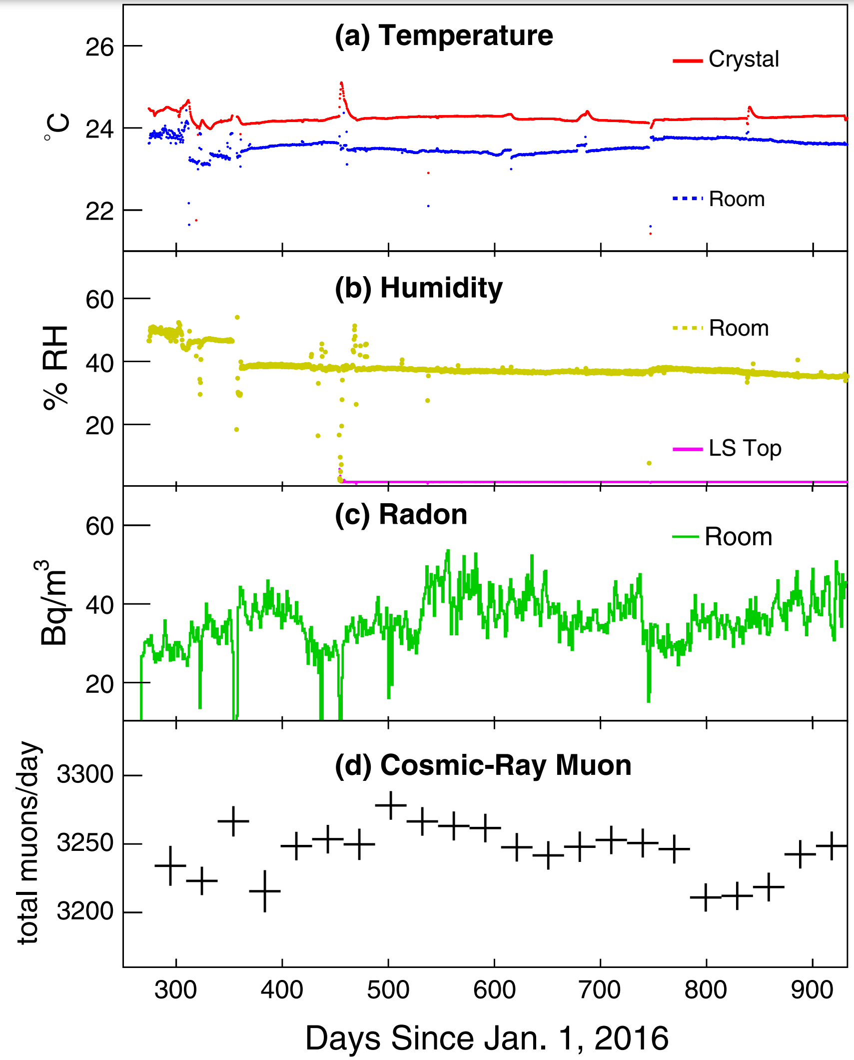

FIG. 1. COSINE-100's environmental parameters as a function of time. (a) Detector room and near-crystal temperature. (b) Relative humidity for the detector room and the top volume of acrylic box, at the top of the LS. Note that the measurement taken at the top of the LS began on day 450. (c) The radon level in the detector room air. (d) Rate of muons passing through the detector over time. Here, the rate is binned in 30-day intervals.

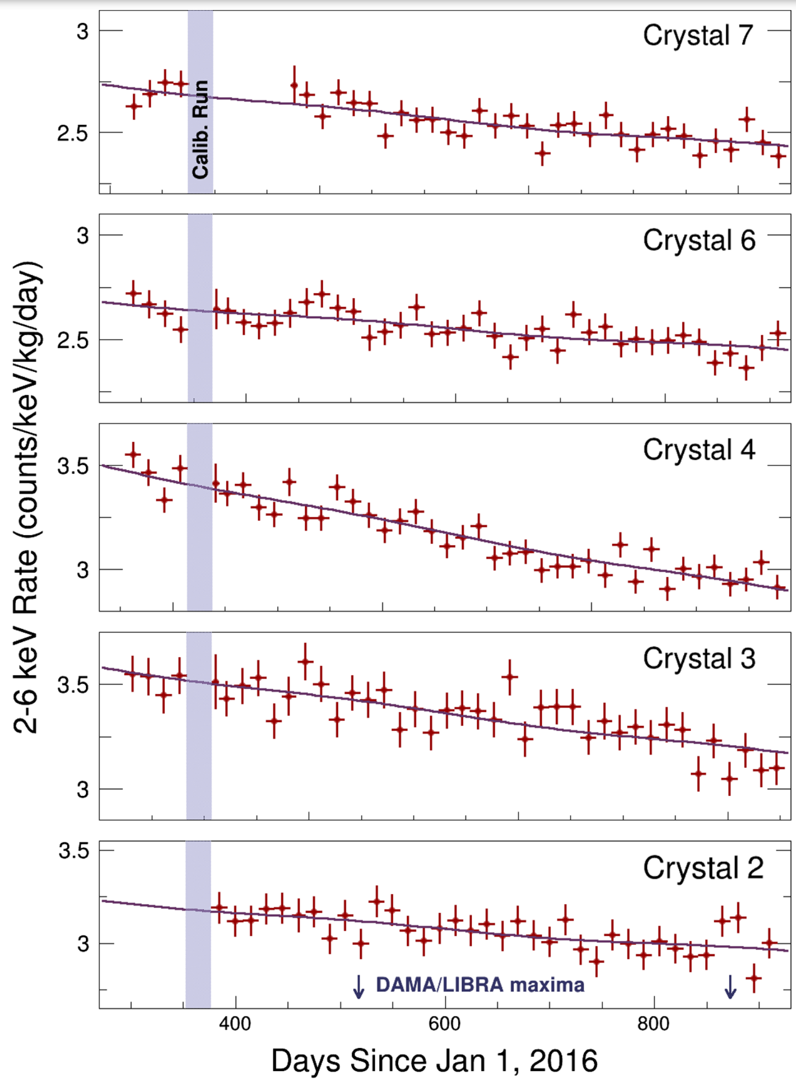

FIG. 3. Rate vs time for Crystals 2, 3, 4, 6, and 7 from October 21, 2016 to July 18, 2018 for the 2–6 keV energy region binned in 15-day intervals. The histograms show the result of the fit described in the text. Solid blue arrows indicate the peak date in the modulation as reported by DAMA/LIBRA [12]. Data taking was suspended for calibrations at the end of 2016 as indicated by the shaded region.

Comparison with DAMA/LIBRA

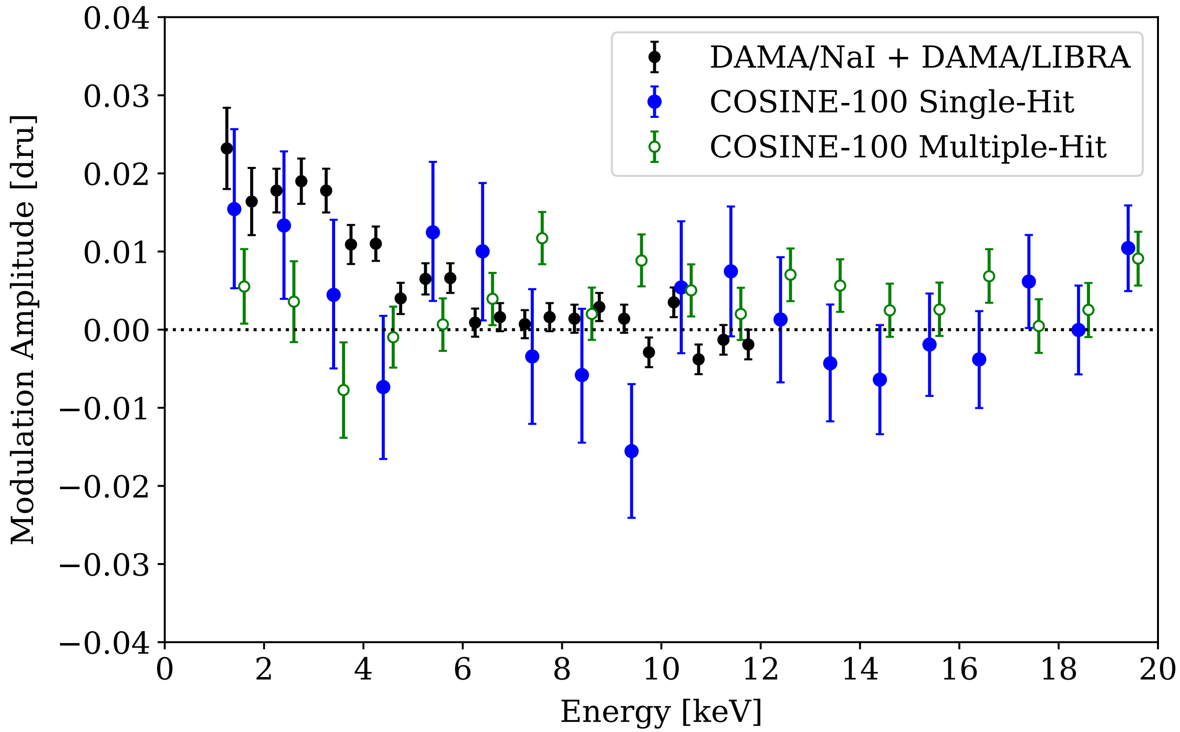

FIG. 8. Measured modulation amplitude as a function of energy in 1 keV bins for the COSINE-100 single-hit (blue closed circles) and multiple-hit (green open circles) datasets. The combined results from DAMA/NaI and DAMA/LIBRA-phase1 and phase2 [13] are also shown for reference. The period and phase of the modulation component are fixed at 365.25 and 152.5 days, respectively. Vertical error bars are the 68.3% highest-density credible intervals of the modulation amplitude posteriors in each energy bin.

G. ADHIKARI et al.
PHYS. REV. D 106, 052005 (2022)

SABRE: NaI modulation check

SABRE North

9 crystals each ~5 kg

fully passive shielding (copper + PE)

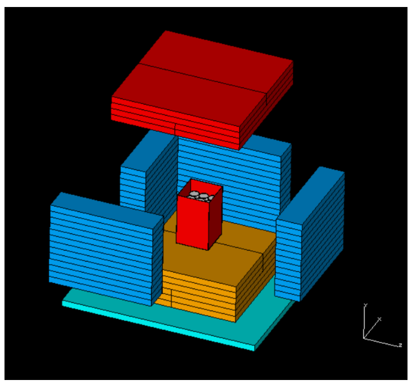

SABRE South

7 crystals, each ~5-7 kg

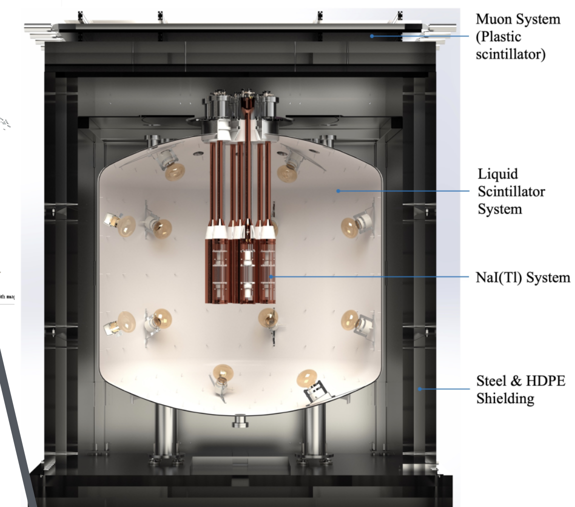

INFN
Istituto Nazionale di Fisica Nucleare

- R&D on ultra-radiopure crystals to reach a lower background than competing experiments.
- TDR approved, entering full scale of experiment

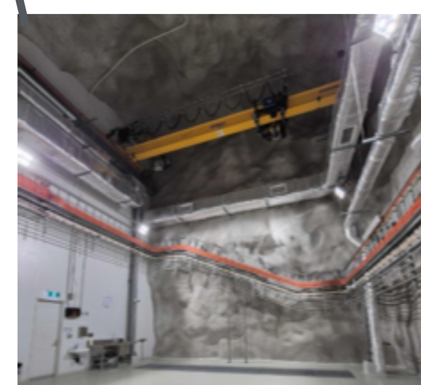

STAWELL UNDERGROUND PHYSICS LAB

NaI quenching factor

Amount of recoil energy going into visible energy

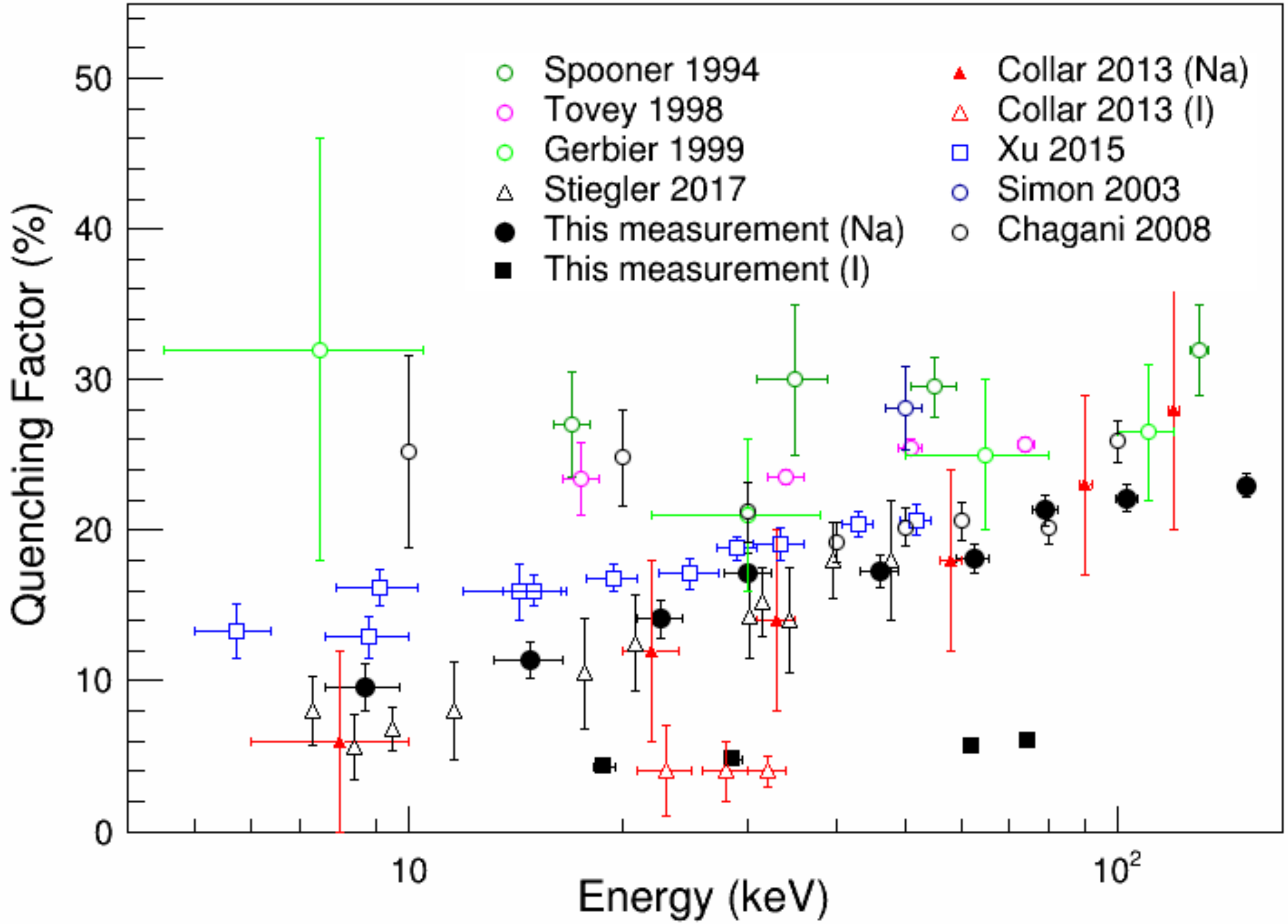

H.W. Joo, et al Astropart Phys, 108 (2019) 50

Cryo-detectors have no quenching:
entire energy eventually converted to phonons